

REPORT DOCUMENTATION PAGE			Form Approved OMB NO. 0704-0188		
<p>The public reporting burden for this collection of information is estimated to average 1 hour per response, including the time for reviewing instructions, searching existing data sources, gathering and maintaining the data needed, and completing and reviewing the collection of information. Send comments regarding this burden estimate or any other aspect of this collection of information, including suggestions for reducing this burden, to Washington Headquarters Services, Directorate for Information Operations and Reports, 1215 Jefferson Davis Highway, Suite 1204, Arlington VA, 22202-4302. Respondents should be aware that notwithstanding any other provision of law, no person shall be subject to any penalty for failing to comply with a collection of information if it does not display a currently valid OMB control number.</p> <p>PLEASE DO NOT RETURN YOUR FORM TO THE ABOVE ADDRESS.</p>					
1. REPORT DATE (DD-MM-YYYY) 10-07-2016		2. REPORT TYPE Final Report		3. DATES COVERED (From - To) 25-Aug-2009 - 24-Feb-2015	
4. TITLE AND SUBTITLE Final Report: Photonic Devices Based on Circuits of Supermonodispersive Spherical Cavities			5a. CONTRACT NUMBER W911NF-09-1-0450		
			5b. GRANT NUMBER		
			5c. PROGRAM ELEMENT NUMBER 611102		
6. AUTHORS Vasily N. Astratov			5d. PROJECT NUMBER		
			5e. TASK NUMBER		
			5f. WORK UNIT NUMBER		
7. PERFORMING ORGANIZATION NAMES AND ADDRESSES University of North Carolina - Charlotte 9201 University City Boulevard Charlotte, NC 28223 -0001			8. PERFORMING ORGANIZATION REPORT NUMBER		
9. SPONSORING/MONITORING AGENCY NAME(S) AND ADDRESS (ES) U.S. Army Research Office P.O. Box 12211 Research Triangle Park, NC 27709-2211			10. SPONSOR/MONITOR'S ACRONYM(S) ARO		
			11. SPONSOR/MONITOR'S REPORT NUMBER(S) 54377-MS.87		
12. DISTRIBUTION AVAILABILITY STATEMENT Approved for Public Release; Distribution Unlimited					
13. SUPPLEMENTARY NOTES The views, opinions and/or findings contained in this report are those of the author(s) and should not be construed as an official Department of the Army position, policy or decision, unless so designated by other documentation.					
14. ABSTRACT This project was devoted to microspherical photonics, a special area at the intersection of optics, photonics and material science, where the optical properties of structures and devices formed by dielectric microsphere are determined by their whispering gallery modes (WGMs) as well by the topological and configuration effects in photonic molecules, microsphere-chain waveguides, and coupled-cavity arrays. The first stage of the project was devoted to understating the basics of the WGM coupling effects in simplest structures such as dielectric bi-spheres. In parallel, we developed understanding of the microsphere chain waveguides based on periodically focusing					
15. SUBJECT TERMS Whispering gallery modes, photonic nanojets, optical forces, laser scalpels, optical super-resolution					
16. SECURITY CLASSIFICATION OF:			17. LIMITATION OF ABSTRACT UU	15. NUMBER OF PAGES	19a. NAME OF RESPONSIBLE PERSON Vasily Astratov
a. REPORT UU	b. ABSTRACT UU	c. THIS PAGE UU			19b. TELEPHONE NUMBER 704-687-8131

Report Title

Final Report: Photonic Devices Based on Circuits of Supermonodispersive Spherical Cavities

ABSTRACT

This project was devoted to microspherical photonics, a special area at the intersection of optics, photonics and material science, where the optical properties of structures and devices formed by dielectric microsphere are determined by their whispering gallery modes (WGMs) as well by the topological and configuration effects in photonic molecules, microsphere-chain waveguides, and coupled-cavity arrays. The first stage of the project was devoted to understating the basics of the WGM coupling effects in simplest structures such as dielectric bi-spheres. In parallel, we developed understanding of the microsphere-chain waveguides based on periodically focusing modes. The second stage of this project was devoted to study of the optical propulsion effects for dielectric microspheres interacting with evanescent electromagnetic fields in liquid suspensions. Here, we observed a giant enhancement of optical forces under resonance with WGMs that opened totally novel way of sorting dielectric microspheres based on their resonant properties. Finally, we assembled resonant coupled-cavity structures and observed spectral manifestations of their coupling and optical transport properties. There were several other directions of research also dealing with the optical properties of dielectric microspheres. These include developing ultra-precise optical scalpels, developing super-resolution imaging applications and enhancing performance of mid-wave infrared photodetectors. The project resulted in multiple patents and device proposals.

Enter List of papers submitted or published that acknowledge ARO support from the start of the project to the date of this printing. List the papers, including journal references, in the following categories:

(a) Papers published in peer-reviewed journals (N/A for none)

<u>Received</u>	<u>Paper</u>
07/05/2016	50 Alexey V. Maslov, Vasily N. Astratov. Microspherical photonics: Sorting resonant photonic atoms by using light, Applied Physics Letters, (09 2014): 121113. doi: 10.1063/1.4895631
07/05/2016	65 Vasily N. Astratov, Yangcheng Li, Oleksiy V. Svitelskiy, Alexey V. Maslov, Michael I. Bakunov, David Carnegie, Edik Rafailov. Microspherical Photonics: Ultra-High Resonant Propulsion Forces, Optics and Photonics News, (): 40. doi:
07/05/2016	66 Yangcheng Li, Alexey V. Maslov, Nicholas I. Limberopoulos, Augustine M. Urbas, Vasily N. Astratov. Spectrally resolved resonant propulsion of dielectric microspheres, Laser & Photonics Reviews, (): 263. doi:
07/05/2016	67 Vasily N. Astratov, Arash Darafsheh, Matthew D. Kerr, Kenneth W. Allen, Nathaniel M. Fried, Andrew N. Antoszyk, and Howard S. Ying. Photonic nanojets for laser surgery, SPIE Newsroom, (): . doi:
07/05/2016	69 Kenneth W. Allen, Navid Farahi, Yangcheng Li, Nicholas I. Limberopoulos, Dennis E. Walker, Augustine M. Urbas, Vasily N. Astratov. Overcoming the diffraction limit of imaging nanoplasmonic arrays by microspheres and microfibers, Optics Express, (): 24484. doi:
07/05/2016	68 Kenneth W. Allen, Navid Farahi, Yangcheng Li, Nicholas I. Limberopoulos, Dennis E. Walker, Augustine M. Urbas, Vladimir Liberman, Vasily N. Astratov. Super-resolution microscopy by movable thin-films with embedded microspheres: Resolution analysis, Annalen der Physik, (): 513. doi:
07/05/2016	70 Kenneth W. Allen, Farzaneh Abolmaali, Joshua M. Duran, Gamini Ariyawansa, Nicholas I. Limberopoulos, Augustine M. Urbas, Vasily N. Astratov. Increasing sensitivity and angle-of-view of mid-wave infrared detectors by integration with dielectric microspheres, Applied Physics Letters, (): 241108. doi:
07/06/2016	71 Seungmoo Yang, Vasily N. Astratov. Spectroscopy of coherently coupled whispering-gallery modes in size-matched bispheres assembled on a substrate, Optics Letters, (): 2057. doi:
07/06/2016	72 Alexey V. Maslov, Vasily N. Astratov. Imaging of sub-wavelength structures radiating coherently near microspheres, Applied Physics Letters, (): 051104. doi:
07/06/2016	73 Vasily N. Astratov, Kenneth W. Allen, Navid Farahi, Yangcheng Li, Nicholas I. Limberopoulos, Dennis E. Walker Jr., Walker, Augustine M. Urbas, Vladimir Liberman, Mordechai Rothschild. Optical nanoscopy with contact microlenses overcomes the diffraction limit, SPIE Newsroom, (): . doi:
TOTAL:	10

Number of Papers published in peer-reviewed journals:

(b) Papers published in non-peer-reviewed journals (N/A for none)

<u>Received</u>	<u>Paper</u>
-----------------	--------------

TOTAL:

Number of Papers published in non peer-reviewed journals:

(c) Presentations

Non Peer-Reviewed Conference Proceeding publications (other than abstracts):

<u>Received</u>	<u>Paper</u>
07/06/2016	74 Yangcheng Li, Farzaneh Abolmaali, Nikolaos I. Limberopoulos, Augustine M. Urbas, Vasily N. Astratov. Coupling properties and sensing applications of photonic molecules, NAECON 2015 - IEEE National Aerospace and Electronics Conference. 14-JUN-15, Dayton, OH, USA. : ,
07/06/2016	75 Farzaneh Abolmaali, Nikolaos I. Limberopoulos, Augustine M. Urbas, Vasily N. Astratov. Observation of the influence of the gain on parity-time-symmetric properties of photonic molecules with coupled whispering gallery modes, NAECON 2015 - IEEE National Aerospace and Electronics Conference. 15-JUN-15, Dayton, OH, USA. : ,
07/06/2016	76 Alexey V. Maslov, Michael I. Bakunov, Vasily N. Astratov. Dynamics of dielectric microparticles in optical fields: Taking advantage of intrinsic particle resonances and hybrid particle-waveguide resonances, 2015 17th International Conference on Transparent Optical Networks (ICTON). 04-JUL-15, Budapest. : ,
07/06/2016	77 Kenneth W. Allen, Navid Farahi, Yangcheng Li, Nikolaos I. Limberopoulos, Dennis E. Walker Jr., Augustine M. Urbas, Vladimir Liberman, Vasily N. Astratov. Super-resolution by microspheres and fibers - Myth or reality?, 2015 17th International Conference on Transparent Optical Networks (ICTON). 05-JUL-15, Budapest. : ,
07/06/2016	78 Kenneth W. Allen, Vladimir Liberman, Mordechai Rothschild, Nikolaos I. Limberopoulos, Dennis E. Walker Jr., Augustine M. Urbas, Vasily N. Astratov. Deep-UV microsphere-assisted ultramicroscopy, 2015 17th International Conference on Transparent Optical Networks (ICTON). 05-JUL-15, Budapest. : ,
07/06/2016	79 V. N. Astratov, A. V. Maslov, K. W. Allen, N. Farahi, Y. Li, A. Brettin, N. I. Limberopoulos, D. E. Walker Jr., A. M. Urbas, V. Liberman, M. Rothschild. Fundamental limits of super-resolution microscopy by dielectric microspheres and microfibers, SPIE BIOS. 12-FEB-16, San Francisco, California, United States. : ,
07/06/2016	80 Arash Darafsheh, Matthew D. Kerr, Kenneth W. Allen, Vasily N. Astratov. Integrated Microsphere Arrays as a Compact Focusing Tool for Biomedical and Photonics Applications, Conference on Lasers and Electro-Optics. 15-MAY-10, San Jose, CA. : ,
07/06/2016	81 Arash Darafsheh, Matthew D. Kerr, Kenneth W. Allen, Nathaniel M. Fried, Andrew N. Antoszyk, Howard S. Ying, and Vasily N. Astratov. Integrated microsphere arrays: light focusing and propagation effects, SPIE OPTO. 26-JAN-10, San Francisco, California. : ,
07/06/2016	82 Arash Darafsheh, Oleksiy V. Svitelskiy, Vasily N. Astratov. Light focusing microprobes for biomedical and photonics applications based on integrated microsphere arrays, 2010 12th International Conference on Transparent Optical Networks (ICTON). 26-JUN-10, Munich, Germany. : ,
TOTAL:	9

Peer-Reviewed Conference Proceeding publications (other than abstracts):

<u>Received</u>	<u>Paper</u>
08/31/2011 6.00	Kenneth W. Allen, Amir Fardad, Nathaniel M. Fried, Andrew N. Antoszyk, Arash Darafsheh, Howard S. Ying, Vasily N. Astratov. Focusing capability of integrated chains of microspheres in the limit of geometrical optics, Laser Resonators and Beam Control XIII. 24-JAN-11, San Francisco, California, USA. : ,
08/31/2011 12.00	Vasily N. Astratov, Arash Darafsheh. Chains of variable size spheres for focusing of multimodal beams in photonics applications, 2011 13th International Conference on Transparent Optical Networks (ICTON). 26-JUN-11, Stockholm, Sweden. : ,
08/31/2011 11.00	Kenneth W. Allen, Arash Darafsheh, Vasily N. Astratov. Photonic nanojet-induced modes: From physics to applications, 2011 13th International Conference on Transparent Optical Networks (ICTON). 26-JUN-11, Stockholm, Sweden. : ,
08/31/2011 10.00	Oleksiy V. Svitelskiy, Yangcheng Li, Misha Sumetsky, David Carnegie, Edik Rafailov, Vasily N. Astratov. A microfluidic platform integrated with tapered optical fiber for studying resonant properties of compact high index microspheres, 2011 13th International Conference on Transparent Optical Networks (ICTON). 26-JUN-11, Stockholm, Sweden. : ,
08/31/2011 9.00	B.D. Jones, M. Oxborrow, V.N. Astratov, M. Hopkinson, A. Tahraoui, M.S. Skolnick, A.M. Fox. Splitting and lasing of whispering gallery modes in quantum dot micropillars, Conference on Lasers and Electrooptics (CLEO). 02-MAY-11, . : ,
08/31/2011 8.00	Amir Fardad, Nathaniel M. Fried, Arash Darafsheh, Andrew N. Antoszyk, Howard S. Ying, Vasily N. Astratov. Ultra-precise focusing multimodal microprobes for contact laser tissue surgery, Conference on Lasers and Electrooptics (CLEO). 02-MAY-11, . : ,
08/31/2011 7.00	Oleksiy Svitelskiy, Dongning Sun, Arash Darafsheh, Mikhail Sumetsky, Anatoly Lupu, Maria Tchernycheva, Vasily N. Astratov. Characterization of high index microsphere resonators in fiber-integrated microfluidic platforms, Laser Resonators and Beam Control XIII. 24-JAN-11, San Francisco, California, USA. : ,
08/31/2012 18.00	Yangcheng Li, Oleksiy V. Svitelskiy, Alexey V. Maslov, David Carnegie, Edik Rafailov, Vasily N. Astratov. Resonant optical propelling of microspheres: A path to selection of almost identical photonic atoms, 2012 14th International Conference on Transparent Optical Networks (ICTON). 02-JUL-12, Coventry, United Kingdom. : ,
08/31/2012 29.00	Arash Darafsheh, Matthew D. Kerr, Kenneth W. Allen, Vasily N. Astratov. Integrated Microsphere Arrays as Compact Focusing Tool for Biomedical and Photonics Applications, OSA / CLEO/QELS 2010. 18-MAY-10, . : ,
08/31/2012 28.00	V.N. Astratov, A. Darafsheh, M.D. Kerr, K.W. Allen, N.M. Fried. Focusing Microprobes Based on Integrated Chains of Microspheres, Progress In Electromagnetics Research Symposium. 07-JUL-10, . : ,
08/31/2012 27.00	Oleksiy V. Svitelskiy, Yangcheng Li, Misha Sumetsky, David Carnegie, Edik Rafailov, Vasily N. Astratov. Resonant coupling to microspheres and light pressure effects in microfluidic fiber-integrated platforms, 2011 IEEE Photonics Conference (IPC). 09-OCT-11, Arlington, VA, USA. : ,

- 08/31/2012 24.00 Thomas C. Hutchens, Arash Darafsheh, Amir Fardad, Andrew N. Antoszyk, Howard S. Ying, Vasily N. Astratov, Nathaniel M. Fried. Novel microsphere chain fiber tips for use in mid-infrared ophthalmic laser surgery, Optical Fibers and Sensors for Medical Diagnostics and Treatment Applications XII. 24-JAN-12, San Francisco, California, USA. : ,
- 08/31/2012 22.00 Kenneth W. Allen, Arash Darafsheh, Vasily N. Astratov. Beam tapering effect in microsphere chains: from geometrical to physical optics, Laser Resonators, Microresonators, and Beam Control XIV. 24-JAN-12, San Francisco, California, USA. : ,
- 08/31/2012 23.00 Yangcheng Li, Oleksiy Svitelskiy, David Carnegie, Edik Rafailov, Vasily N. Astratov. Evanescent light coupling and optical propelling of microspheres in water immersed fiber couplers, Laser Resonators, Microresonators, and Beam Control XIV. 24-JAN-12, San Francisco, California, USA. : ,
- 08/31/2012 21.00 Arash Darafsheh, Anatole Lupu, S. A. Burand, Thomas C. Hutchens, Nathaniel M. Fried, Vasily N. Astratov. Photonic nanojet-induced modes: fundamentals and applications, Integrated Optics: Devices, Materials, and Technologies XVI. 24-JAN-12, San Francisco, California, USA. : ,
- 08/31/2012 20.00 Arash Darafsheh, Michael A. Fiddy, Vasily N. Astratov. Super-resolution imaging by high-index microspheres immersed in a liquid, 2012 14th International Conference on Transparent Optical Networks (ICTON). 02-JUL-12, Coventry, United Kingdom. : ,
- 08/31/2012 19.00 Arash Darafsheh, Vasily N. Astratov. Radial polarization of periodically focused modes in chains of dielectric spheres, 2012 14th International Conference on Transparent Optical Networks (ICTON). 02-JUL-12, Coventry, United Kingdom. : ,
- 10/05/2014 55.00 Yangcheng Li, Kenneth W. Allen, Farzaneh Abolmaali, Alexey V. Maslov, Vasily N. Astratov. Spectral finger-prints of photonic molecules, 2014 16th International Conference on Transparent Optical Networks (ICTON). 06-JUL-14, Graz, Austria. : ,
- 10/05/2014 63.00 Yangcheng Li, Alexey V. Maslov, Nikolaos I. Limberopoulos, Vasily N. Astratov. Demonstration of whispering-gallery-mode resonant enhancement of optical forces, National Aerospace and Electronic Conference (NAECON). 25-JUN-14, . : ,
- 10/05/2014 62.00 Kenneth W. Allen, Navid Farahi, Yangcheng Li, Nikolaos I. Limberopoulos, Dennis E. Walker Jr., Augustine M. Urbas, Vasily N. Astratov. Super-resolution imaging by arrays of high-index spheres embedded in transparent matrices, National Aerospace and Electronic Conference (NAECON). 25-JUN-14, . : ,
- 10/05/2014 61.00 Kenneth W. Allen, Joshua M. Duran, Gamini Ariyawansa, Jarrett H. Vella, Nikolaos I. Limberopoulos, Augustine M. Urbas, Vasily N. Astratov. Photonic Jets for Strained-Layer Superlattice Infrared Photodetector Enhancement, National Aerospace and Electronic Conference (NAECON) . 25-JUN-14, . : ,
- 10/05/2014 60.00 Yangcheng Li, Alexey V. Maslov, Vasily N. Astratov. Spectral control and temporal properties of resonant optical propulsion of dielectric microspheres in evanescent fiber couplers, SPIE LASE. 01-FEB-14, San Francisco, California, United States. : ,
- 10/05/2014 57.00 Michael I. Bakunov, Yangcheng Li, Vasily N. Astratov, Alexey V. Maslov. Resonant optical forces associated with the excitation of whispering gallery modes in microparticles, 2014 16th International Conference on Transparent Optical Networks (ICTON). 06-JUL-14, Graz, Austria. : ,

- 11/04/2013 42.00 Yangcheng Li, Alexey V. Maslov, Ana Jofre, Vasily N. Astratov. Tuning the optical forces on- and off-resonance in microspherical photonics, 2013 15th International Conference on Transparent Optical Networks (ICTON). 23-JUN-13, Cartagena, Spain. : ,
- 11/04/2013 34.00 Yangcheng Li, Alexey V. Maslov, Oleksiy Svitelskiy, David Carnegie, Edik Rafailov, Vasily N. Astratov. Giant Resonant Light Forces in Microspherical Photonics, CLEO: Science and Innovations. 10-JUN-13, San Jose, California. : ,
- 11/04/2013 36.00 Alexey F. Kosolapov, Anton N. Kolyadin, Andrey D. Pryamikov, Neda Mojaverian, Nicholaos I. Limberopoulos, Vasily N. Astratov, Kenneth W. Allen. Photonic jets produced by microspheres integrated with hollow-core fibers for ultraprecise laser surgery, 2013 15th International Conference on Transparent Optical Networks (ICTON). 23-JUN-13, Cartagena, Spain. : ,
- 11/04/2013 37.00 Arash Darafsheh, Nicholaos I. Limberopoulos, John S. Derov, Dennis E. Walker, Vasily N. Astratov. Comparison between microsphere-assisted and confocal microscopies, 2013 15th International Conference on Transparent Optical Networks (ICTON). 23-JUN-13, Cartagena, Spain. : ,
- 11/04/2013 39.00 Yangcheng Li, Vasily N. Astratov, Arash Darafsheh. Super-resolution microscopy by dielectric microcylinders, 2013 15th International Conference on Transparent Optical Networks (ICTON). 23-JUN-13, Cartagena, Spain. : ,
- 11/05/2013 43.00 Arash Darafsheh, Nicholaos I. Limberopoulos, John S. Derov, Dennis E. Walker, Magdalena Durska, Dmitry N. Krizhanovskii, David M. Whittaker, Vasily N. Astratov, Alexander N. Cartwright, Dan V. Nicolau. Optical microscopy with super-resolution by liquid-immersed high-index microspheres, SPIE BIOS. 04-FEB-13, San Francisco, California, USA. : ,
- 11/05/2013 44.00 Arash Darafsheh, Thomas C. Hutchens, Amir Fardad, Andrew N. Antoszyk, Howard S. Ying, Nathaniel M. Fried, Vasily N. Astratov. Contact focusing multimodal probes for potential use in ophthalmic surgery with the Erbium:YAG laser, SPIE BIOS. 04-FEB-13, San Francisco, California, USA. : ,
- 11/05/2013 45.00 Arash Darafsheh, Nicholaos I. Limberopoulos, Anatole Lupu, Vasily N. Astratov. Filtering of radially polarized beams by microsphere-chain waveguides, SPIE OPTO. 04-FEB-13, San Francisco, California, USA. : ,

TOTAL: 31

Number of Peer-Reviewed Conference Proceeding publications (other than abstracts):

(d) Manuscripts

<u>Received</u>	<u>Paper</u>
-----------------	--------------

TOTAL:

Books

Received Book

TOTAL:

Received Book Chapter

07/06/2016 83.00 Vasily N. Astratov. Fundamentals and Applications of Microsphere Resonator Circuits, : Springer Series in Optical Sciences, (2010)

TOTAL: 1

Patents Submitted

- 1. Methods and Systems for Enhancing the Performance of Photodetector Focal Plane Arrays
~~V.N. Astratov, K.W. Allen, N.I. Limberopoulos, A. Urbas, and J. M. Duran, patent application 14/587,068 filed on~~
12/31/2014. U.S. patent 9,362,324 (7 June 2016)
- 2. Contact Focusing Hollow-Core Fiber Microprobes
V.N. Astratov, U.S. patent application 2015/0316717 A1 published on November 5, 2015, related to U.S. provisional application 61/728,835 filed on 11/21/2012.
- 3. Methods and Systems for Super-Resolution Optical Imaging Using High-Index of Refraction Microspheres and Microcylinders
V.N. Astratov and A. Darafsheh, US patent application 2014/0355108 A1 published on December 4, 2014, related to U.S. provisional application 61/656,710 filed on June 07, 2012.
- 4. Methods and Devices for Optical Sorting of Microspheres Based on Their Resonant Optical Properties
V.N. Astratov, US patent application 2014/0069850 A1 published on 13 March 2014 related to U.S. provisional application 61/535,409 filed on September 16, 2011. U.S. patent 9242248 B2 (26 January 2016).
- 5. Focusing multimodal optical microprobe devices and methods
V.N. Astratov, U.S. patent 8,554,031 B2 published on 08 October 2013 (priority date January 17, 2009). Also published as EP2443494A1, US20120091369, WO2011005397A1.

Patents Awarded

1. Methods and Systems for Enhancing the Performance of Photodetector Focal Plane Arrays

~~V.N. Astratov, K.W. Allen, N.I. Limberopoulos, A. Urbas, and J. M. Duran, patent application 14/587,068 filed on 12/31/2014. U.S. patent 9,362,324 (7 June 2016)~~

2. Contact Focusing Hollow-Core Fiber Microprobes

V.N. Astratov, U.S. patent application 2015/0316717 A1 published on November 5, 2015, related to U.S. provisional application 61/728,835 filed on 11/21/2012.

3. Methods and Systems for Super-Resolution Optical Imaging Using High-Index of Refraction Microspheres and Microcylinders

V.N. Astratov and A. Darafsheh, US patent application 2014/0355108 A1 published on December 4, 2014, related to U.S. provisional application 61/656,710 filed on June 07, 2012.

4. Methods and Devices for Optical Sorting of Microspheres Based on Their Resonant Optical Properties

V.N. Astratov, US patent application 2014/0069850 A1 published on 13 March 2014 related to U.S. provisional application 61/535,409 filed on September 16, 2011. U.S. patent 9242248 B2 (26 January 2016).

5. Focusing multimodal optical microprobe devices and methods

V.N. Astratov, U.S. patent 8,554,031 B2 published on 08 October 2013 (priority date January 17, 2009). Also published as EP2443494A1, US20120091369, WO2011005397A1.

Awards

1. NIH Grant: In March 2010 the PI was awarded NIH STTR Phase I grant, "Novel Optical Microprobes for Ultra-Precise Intraocular Laser Surgery," totaling \$222,416.
2. UNCC Research Award: In January 2009 the PI's Faculty Grant Proposal "High Resolution Optical Microprobe for Laser Surgery" has been awarded a grant totaling \$6,000.
3. The PI was a co-organizer of a Special session "Microresonators and Photonic Molecules" at the international conference on transparent networks (ICTON'09) which was held in Island of São Miguel, Azores, Portugal, on June 28-July 2 (2009).
4. The PI was a chair at one of the sessions at the international conference on transparent networks (ICTON'09) which was held in Island of São Miguel, Azores, Portugal, on June 28-July 2 (2009).
5. The PI was an invited speaker at a Special session "Microresonators and Photonic Molecules" at the international conference on transparent networks (ICTON'10) which was held in Munich, Germany, on June 27-July 1 (2010).
6. The PI was a chair at one of the sessions at the international conference on transparent networks (ICTON'10) which was held in Munich, Germany, on June 27-July 1 (2010).
7. The PI's former PhD student, Seungmoo Yang, was awarded a postdoctoral position at Northwestern University after graduation with PhD thesis from UNC-Charlotte in July 2009.
8. In November 2009 the PI was invited to submit an article to SPIE Newsroom, an international internet journal highlighting developments in the area of photonics.
9. The PI was invited to give an invited talk at Photonics West 2010 which was held in San Francisco on January 23-28, 2010.
10. The PI was invited to give an invited talk at major international conference PIERS 2010 which was held in Cambridge in July 5-8, 2010.
11. The PI was invited to give a talk at University of Paris XI, Institute of Fundamental Electronics, June 23, 2010, host: A. Lupu. Title: "Microsphere Resonator Arrays for Photonics and Biomedical Optics Applications."
12. The PI was invited to give a talk at Institute Fresnel, Aix-Marseille University, Marseille, France, June 24, 2010, host: N. Bonod. Title: "Microsphere Resonator Arrays for Photonics and Biomedical Optics Applications."
13. The PI was invited to give a talk at Walter Schottky Institute, Munich, July 2, 2010, host: Jonathan Finley. Title: "Microsphere Resonator Arrays for Photonics and Biomedical Optics Applications."
14. The PI was invited to give a talk at Boston University, Boston, July 5, 2010, host: Luca Dal Negro. Title: "Fundamentals and Applications of Microsphere Resonator Arrays."
15. ARO DURIP Award on 07/21/2011: Tunable Light Source for Observation of Novel Effects of Resonant Light Pressure and Development of Microsphere Resonator Circuits, sole PI (V.N. Astratov), Total \$192,000
16. The UNC and the State Board of Community Colleges Equipment Grant on 01/01/2011: Infrared Imaging System for Characterization of the Optical Scalpel Structures, PI (V.N. Astratov), Total \$32,000
17. Membership (V.N. Astratov) in Management Committee of a major European scientific organization, European Cooperation on Science and Technology (COST) since December 2009 within COST Action MP0702 "Towards Functional Sub-Wavelength Photonic Structures."
18. International Visiting Award in France by Triangle de la Physique to visit three major photonics laboratories in France in June 2011: i) Institute for Fundamental Electronics, University Paris Sud XI, ii) Laboratoire Charles Fabry de l'Institut d'Optique, and iii) Laboratoire de Photonique et Nanostructures LPN-CNRS.
19. Guest Editor (V.N. Astratov), Focus Issue of Optics Express, Collective Phenomena in Photonic, Plasmonic and Hybrid Structures, Nov. 2011
20. Alternate chair (V.N. Astratov) of the program subcommittee, Int. Conf. on Lasers and Electrooptics (CLEO'12), subcommittee Micro and Nano-Photonic Devices
21. Chair of Microresonators and Photonic Molecules Session at Int. Conf. on transparent networks (ICTON'11),

Stockholm, Sweden, June

26-30 (2010).

22. Invited talk (V.N. Astratov) at major international conference ICTON'11, Stockholm, Sweden, June 26-30 (2011):

"Photonic nanojet-induced modes: from physics to applications"

23. Chair of Special Symposium on Innovative Optical Microresonators V at IEEE Photonics 2011 (Formerly LEOS), 9-13 October,

Arlington, Virginia

24. Invited talk (V.N. Astratov) at major conference IEEE Photonics 2011 (Formerly LEOS), 9-13 October, Arlington, Virginia:

"Resonant coupling to microspheres and light pressure effects in microfluidic fiber-integrated platforms"

25. Invited speaker at the NSF ECCS Grantees Meeting, Honolulu, U.S.A., November 30-December 2, 2010:

"Mesoscale Structures and Photonic Devices based on Coupled Spherical Cavities."

26. The PI gave an invited talk at LTM-CNRS, Grenoble, France, June 20, 2011, host: David Peyrade

"Microsphere Circuits for Photonics and Biomedical Applications"

27. The PI gave an invited talk at West Virginia University, Morgantown, October 22, 2010, host: Alan Bristow

"Fundamentals and Applications of Microsphere Resonator Arrays"

28. ARO DURIP Award on 06/28/2012: Ultrahigh Resolution Broadband Spectroscopic System for Investigation of Microsphere Resonator Circuits, DURIP, Proposal No. 61475-MS-RIP, Army Research Office, Sole PI (V.N. Astratov), Total award \$60,255.

29. Alternate Chair, program committee, CLEO 2012, Micro- and Nano-Photonic Devices.

30. In July 2012 the PI was invited to be an Alternate Chair, program committee, CLEO 2013, Micro- and Nano-Photonic Devices.

31. In February 2012 the PI worked as a panelist for National Science Foundation, DMR CMP 2012.

32. Chair of Microresonators and Photonic Molecules Session at Int. Conf. on transparent networks (ICTON'12), Coventry, U.K., July 2-5 (2012).

33. Invited talk (V.N. Astratov): International conference ICTON'12, Coventry, U.K., July 2-5 (2012): "Resonant Optical Propelling of Microspheres – A Path to Selection of Almost Identical Photonics Atoms"

34. Invited talk (V.N. Astratov): University of Sheffield, UK, July 9, 2012, host Maurice Skolnick, "Microspherical Photonics: From Nanojets to Resonant Light Pressure and Optical Super-Resolution Effects"

35. The PI was invited to visit WP AFB in July 16-July 27, 2012.

36. Invited talk (V.N. Astratov): AFRL/RX on July 25 2012, host Ilya Vitebskiy, "Microspherical Photonics: From Nanojets to Resonant Light Pressure and Optical Super-Resolution Effects"

37. Graduate student in the PI's group, Arash Darafsheh, obtained a prestigious summer fellowship and internship at NASA (the Langley Aerospace Research Student Scholars (LARSS) Program).

38. News Highlight about observation of resonant optical forces in microspherical photonics will be published in December Issue of Optics and Photonics News in 2013.

39. Chair, One of the opto-mechanical sessions at CLEO 2013

40. Chair, Photonic molecule session at ICTON 2013

41. Invited speaker, ICTON 2013

42. Invited speaker, AFRL/RX Colloquium, WPAFB, Dayton, OH, May 1, 2013, host: Augustin Urbas

43. Invited speaker, University of Texas at San Antonio, San Antonio, TX, November 30, 2012, host: Andrey Chabanov

44. AFRL/RX Colloquium, WPAFB, Dayton, OH, July 25, 2012, host: Ilya Vitebskiy

45. Panelist, NSF: DMR CMP 2012

46. Panelist, NSF: SBIR ENG/IIP 2013

47. Program Subcommittee Member, CLEO 2012-2014, Micro- and Nano-Photonic Devices

48. Program Subcommittee Member, IEEE IPC 2014, Optical Micro/Nano Resonators and Devices

49. Program Subcommittee Member, OECC/ACOFT Frontiers in Photonics 2014

50. Program Committee Member, HONET 2012-2014

51. My PhD student, Arash Darafsheh, was awarded NASA Langley Aerospace Research Student Scholars (LARSS) internship: July-August 2012.

52. My PhD student, Arash Darafsheh, after graduation with PhD in May 2012 obtained postdoctoral position at the University of Pennsylvania.

Graduate Students

NAME	PERCENT SUPPORTED	Discipline
Kenneth Allen	0.40	
Yangcheng Li	0.40	
Arash Darafsheh	0.40	
FTE Equivalent:	1.20	
Total Number:	3	

Names of Post Doctorates

<u>NAME</u>	<u>PERCENT SUPPORTED</u>
Oleksiy Svitelskiy	0.50
FTE Equivalent:	0.50
Total Number:	1

Names of Faculty Supported

<u>NAME</u>	<u>PERCENT SUPPORTED</u>	National Academy Member
Vasily Astratov	0.10	
FTE Equivalent:	0.10	
Total Number:	1	

Names of Under Graduate students supported

<u>NAME</u>	<u>PERCENT SUPPORTED</u>	Discipline
Dongning Sun	0.05	Civil Engineering
Danielle Delgado	0.00	Physics
Kenneth Allen	0.05	Physics
FTE Equivalent:	0.10	
Total Number:	3	

Student Metrics

This section only applies to graduating undergraduates supported by this agreement in this reporting period

The number of undergraduates funded by this agreement who graduated during this period: 3.00

The number of undergraduates funded by this agreement who graduated during this period with a degree in science, mathematics, engineering, or technology fields:..... 3.00

The number of undergraduates funded by your agreement who graduated during this period and will continue to pursue a graduate or Ph.D. degree in science, mathematics, engineering, or technology fields:..... 2.00

Number of graduating undergraduates who achieved a 3.5 GPA to 4.0 (4.0 max scale):..... 2.00

Number of graduating undergraduates funded by a DoD funded Center of Excellence grant for Education, Research and Engineering:..... 0.00

The number of undergraduates funded by your agreement who graduated during this period and intend to work for the Department of Defense 1.00

The number of undergraduates funded by your agreement who graduated during this period and will receive scholarships or fellowships for further studies in science, mathematics, engineering or technology fields:..... 2.00

Names of Personnel receiving masters degrees

<u>NAME</u>	
Kenneth Allen	
Adam Burand	
Navid Farahi	
Total Number:	3

Names of personnel receiving PhDs

<u>NAME</u> Seungmoo Yang Arash Darafsheh Kenneth Allen Yangcheng Li Total Number:	 4
--	-----------------------

Names of other research staff

<u>NAME</u>	<u>PERCENT SUPPORTED</u>
FTE Equivalent:	
Total Number:	

Sub Contractors (DD882)

Inventions (DD882)

5 Contact Focusing Hollow-Core Fiber Microprobes

Patent Filed in US? (5d-1) Y

Patent Filed in Foreign Countries? (5d-2) N

Was the assignment forwarded to the contracting officer? (5e) Y

Foreign Countries of application (5g-2):

5a: Vasily Astratov

5f-1a: University of North Carolina at Charlotte

5f-c: 9201 University City Blvd

Charlotte NC 28223

5 Methods and Devices for Optical Sorting of Size-Matched Microspheres

Patent Filed in US? (5d-1) Y

Patent Filed in Foreign Countries? (5d-2) N

Was the assignment forwarded to the contracting officer? (5e) Y

Foreign Countries of application (5g-2):

5a: Vasily Astratov

5f-1a: University of North Carolina at Charlotte

5f-c: 9201 University City Blvd

Charlotte NC 28223

5 Methods and Systems for Enhancing the Performance of Photodetector Focal Plane Arrays

Patent Filed in US? (5d-1) Y

Patent Filed in Foreign Countries? (5d-2) N

Was the assignment forwarded to the contracting officer? (5e) Y

Foreign Countries of application (5g-2):

5a: Vasily Astratov et al

5f-1a: University of North Carolina at Charlotte

5f-c: 9201 University City Blvd

Charlotte NC 28223

Scientific Progress

Technology Transfer

The technology of focusing multimodal microprobes has a commercialization potential. The collaborative research on application of novel optical scalpels in retinal surgery is started with Dr. Howard Ying, an assistant professor of ophthalmology in the Wilmer Eye Institute and Applied Physics Laboratory at Johns Hopkins University. Similar collaborative effort is started with Dr. Andrew Antoszyk, a vitreoretinal surgeon at Charlotte Eye Ear Nose and Throat Associates. At the present stage we plan further ex-vivo testing of our scalpels using infrared medical lasers in collaboration with Dr. Nathaniel Fried's biomedical optics group in our department at UNC-Charlotte.

The super-resolution technology has a strong commercialization potential. The nanoplasmonic arrays for super-resolution studies were fabricated at AFRL and passed to my lab. The development of this technology took place in strong interaction with AFRL scientists, Drs. Nicholas Limberopoulos and Augustine Urbas. Imaging of nanoplasmonic arrays as well as biomedical structures is ultimately suitable for developing business-oriented SBIR/STTR projects. Currently, we have plans of creating a start-up company based on our results.

I. COVER PAGE

Grant No. W911NF-09-1-0450, Proposal No. 54377-MS

Final Report

Photonic Devices Based on Circuits of Supermonodispersive Spherical Cavities

Vasily N. Astratov

Period of performance August 25, 2009 – February 24, 2015

Technical Point of Contact

University of North Carolina – Charlotte:

V.N. Astratov

Department of Physics and Optical Science

9201 University City Blvd.,

Charlotte, NC 28223-0001

Tel: (704) 687-8131

Fax: (704) 687-8197

E-mail: astratov@uncc.edu

TABLE OF CONTENTS

1. Statement of the Problems Studied	3
1.1. Background	4
1.2. Objectives	5
2. Resonant Coupling in Bispheres	6
3. Whispering Gallery Modes in Semiconductor Micropillars	7
4. Tapered Fiber-to-Microsphere Couplers	8
5. Observation and Study Resonant Light Forces	9
6. Spectral Fingerprints of Photonic Molecules	13
7. Microsphere-chain waveguides	16
7.1 Transport and focusing properties	17
7.2 Polarization properties	20
7.3 Laser-surgery applications	23
8. Super-Resolution by Microspheres	27
9. Enhancement of Sensitivity and Angle-of-View of Mid-IR Detectors	31
10. Summary and Outlook	34
11. Bibliography	36

1. Statement of the Problems Studied

The main thrust of this ARO project was devoted to developing technology of sorting microspherical resonators with extraordinary uniform spectral positions of their whispering gallery mode (WGM) resonances and demonstration of coupled-cavity structures and devices built from such extremely uniform building blocks. Developing this technology in this project led to a significant breakthrough in physical understanding of the light forces which can be evanescently exerted on dielectric microspheres. New effect of giant resonant enhancement of the light forces was observed in the experiments with the optical propulsion of polystyrene microspheres in the water-immersed fiber couplers. This effect opens new ways of optical sorting microspheres by focused laser beams which can be performed in air or liquid environment. In this project, we demonstrated the utility of the proposed method and realized many coupled-cavity structures formed by multiple spheres with resonant WGMs. We tested the optical properties and performance of such photonic clusters or molecules using side coupling by tapered microfiber connected with a broadband tunable spectroscopic system YENISTA, which was acquired through DURIP awards W911NF-11-1-0406 and W911NF-12-1-0538. These studies revealed that the photonic molecules built from such uniform atoms have spectral properties (such as the spectral WGM splitting) which are dependent on the number and spatial configuration of the coupled resonators. We studied these spectral signatures in different structures and found good agreement between measured and calculated spectra.

Besides resonant properties determined by WGM resonances, we studied many other optical properties of individual microspheres, chains of spheres and microspherical arrays. An example of such research is represented by *super-resolution imaging* of nanoplasmonic and other structures by high-index liquid-immersed spheres. More recently, we suggested and developed technology of embedding such high-index microspheres in transparent elastomeric slabs or coverslips. These results have important applications in nanophotonics and biomedical imaging since they can boost the resolution of conventional microscopes beyond the diffraction limit.

We also studied the optical transport and focusing properties of microsphere-chain waveguides as well as applications of such structures in polarizers and optical scalpels for precise laser surgery. We also studied applications of microspheres as focusing microlenses increasing sensitivity of angle-of-view of mid-IR photodetectors. Finally, in Section 5 of this report we present summary of the results and the outlook for future work.

1.1. Background

Dielectric microspheres became an increasingly important building block and object of studies in mesoscale photonics. Traditional optical applications of microspheres include their use as microlenses and as additives increasing the paint reflecting properties for highway safety. In recent years, however, the microspheres became a holy grail of mesoscale photonics because of the properties of photonic nanojets and nanojet-induced modes, WGMs, and super-resolution imaging applications. The range of applications of such structures and devices is truly extraordinary, spanning the areas from advanced imaging to sensing applications. Microspheres can be also used as building blocks of metamaterial structures and devices.

Structures formed by the optically coupled microsphere can be also considered as a class of metamaterials, especially if the microspheres are integrated with nonlinear materials, photonics crystals, or nanoplasmonic structures.¹ Technologically, the microspherical photonics is very diverse and reach area since there are many different technologies of producing microspheres made from materials with different index of refraction and with different optical properties. The examples include emulsion-based synthesis, cluster aggregation reaction in colloidal solutions, melting the tip of the fibers, and other technologies. Mother Nature prefers the spherical shape and smoothness of the surface due to minimization of the surface energy. For these reasons, microspheres often demonstrate in optical experiments precious properties of dielectric objects with perfect shape. Microspheres are inexpensive and they can be synthesized in massive quantities. They can be also easily integrated with various active and nonlinear structures and materials. Microspheres usually have extraordinary smooth surface and they provide many freedoms in metamaterials and general microphotonics designs due to a range of indices available, established core-shell syntheses technologies, and developed techniques of directed self-assembly of microspheres in chip-scale structures.

The PI, Dr. Vasily N. Astratov [VNA], has a unique expertise and achievements in developing microspherical photonics. In 1995 he pioneered synthetic opals as new class of self-assembled photonic crystals.²⁻⁷ The structure of opals is formed by silica nanospheres packed in a 3D lattice with the face-centered-cubic symmetry. This work changed the direction of the world-wide research in photonic crystals and resulted in a race for 3D photonic crystals with a complete photonic band gap. In 1997-2002 he developed new spectroscopic techniques of characterization of photonic crystal waveguides⁸⁻¹⁴ and semiconductor microcavities¹⁵⁻¹⁸.

Since 2002 the PI's group at UNC-Charlotte initiated studies of optical transport in long chains,^{19,20} clusters,^{21,22} and 3D crystal-like structures²³ of coupled resonators. It should be noted that similar structures formed by micro-rings,^{24,25,26} disks, and toroids can be fabricated by various techniques. However, the microspheres are different from other cavities in a sense that they can be individually micromanipulated and integrated in different structures by using methods of directed self-assembly or forced assembly. In his group [VNA] has (i) observed long-range optical transport due to coupling between whispering gallery modes (WGMs) in size-disordered spheres¹⁹, (ii) studied efficiency of coupling between size-mismatched spheres,²¹ and (iii) introduced a concept of percolation of light in disordered structures with different dimensionality.²³ In 2007-2008, the PI's group observed quasi-periodic modes in chains of spheres which were termed photonic "nanojet-induced modes" (NIMs)^{27,28} based on analogy with "photonic nanojets"^{29,30} – tightly focused beams formed by the individual spheres.

1.2. Objectives

This project has several directions of research covering all aspects of microspherical photonics. It was performed during August 2009-February 2015 period and included the following objectives:

- a) Task 1: Understand basic physics of WGM coupling effects in dielectric bi-spheres as simplest example of coupled-cavity structures.
- b) Task 2: Developing evanescent tapered-fiber couplers and characterized coupling to WGMs in high-index spheres in a water and air environments.
- c) Task 3: Study of new way of manipulation and propulsion of microspheres using resonant light forces. Developing novel methods of sorting spheres based on using resonant light forces.
- d) Task 4: Demonstration of the optical functionality of the circuits formed by spheres with resonant WGM peak positions. To achieve this goal, our project was extended.
- e) Task 5: Demonstration and study of microsphere-chain waveguides including transport, focusing and polarization properties.
- f) Task 6: Developing laser-surgery applications of photonic nanojets.
- g) Task 7: Observation and study of super-resolution imaging applications of microspherical photonics.
- h) Task 8: Integration of microspheres with mid-wave infrared photodetectors and imagers.

2. Resonant Coupling in Bispheres

Coupling in bispheres is a special case since two spheres with almost identical resonant properties can in principle be selected using micromanipulation in combination with spectroscopic characterization.³¹ At the initial stage of our project our goal was to understand the efficiency and basic spectral properties of WGM coupling effects, so we decided to use micromanipulation as the only available way of sorting resonant microspheres at that time. The techniques of micromanipulation by a tapered microfiber and typical fluorescence (FL) spectrum with WGM emission peaks are illustrated in Fig. 1. WGM coupling effects were detected due to splitting effects observed for resonant polystyrene spheres with diameters in a 3-7 μm range. It was shown that coupling is provided between the fundamental WGMs oriented in the equatorial plane of spheres on a substrate, see Fig. 1. Based on these results, the coupling constant (κ) was quantified as a function of the sphere diameter, as shown in Fig. 2. These results, generally, show the feasibility of developing coupled-resonator optical waveguides (CROW) or photonic molecules, where many WGMs can be resonantly coupled. However, they also show that for achieving efficient coupling the variations of the spheres diameters in such circuits should be within the accuracy determined by parameter κ which typically has value $\sim 10^{-3}$, as illustrated in Fig. 2. This means that the commercial microspheres which have size dispersion limited by $\sim 10^{-2}$ cannot be used for developing microsphere resonator circuits and a different technological approach or physical principle for sorting resonant microspheres should be developed.

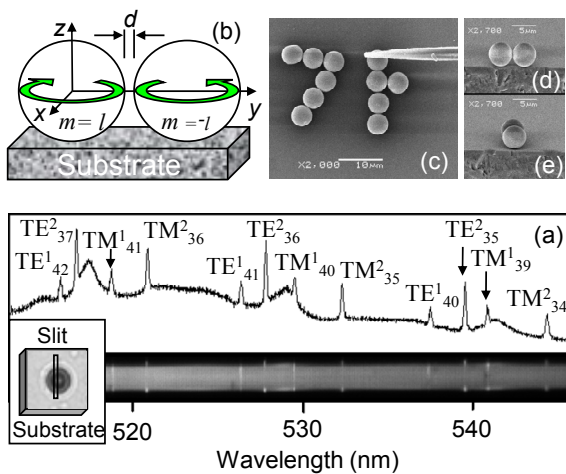


Fig. 1. (a) FL spectrum with WGM peaks, (b) schematic of bisphere, (c) micromanipulation, and (d,e) different orientations of bispheres.

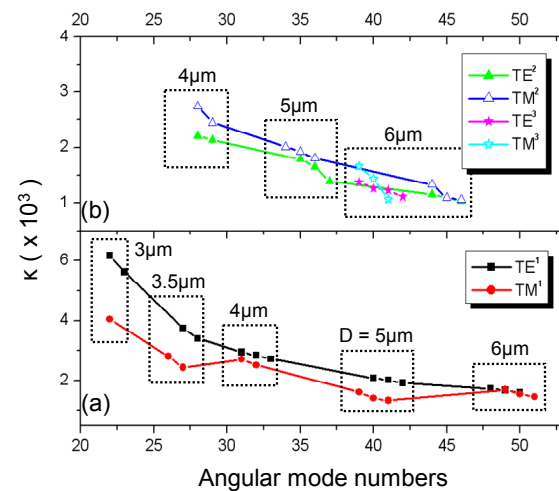


Fig. 2. Coupling constant (κ) for sphere diameters in 3-5 μm range for (a) first- and (b) second-order (radial) WGMs.

3. Whispering gallery modes in semiconductor micropillars

At the same time, we decided to study an alternative approach to developing coupled resonator waveguides based on using established semiconductor technology which allows fabrication semiconductor micropillars, as shown in Fig. 3. The structure contained two multilayer Bragg mirrors with an active layer of InAs quantum dots grown in the middle of the cavity. Such structures were previously used for studying light-matter interaction for the modes confined by the Bragg mirrors. In such structures we observed WGM-based lasing.^{32,33} Multimode lasing with very low thresholds and high β -factors approaching unity was observed under optical pumping in GaAs/AlGaAs pillars with diameters from 4 to 20 μm , see Fig. 3 (a). It was found that WGMs photoluminescence peaks observed from some of the 5 μm and all of the 20 μm pillars were split into doublets shown in Fig. 3 (b). The splitting appears to be intrinsic to the structure, and varies strongly with the wavelength, which is consistent with the model in which the quantum dots themselves act as resonant scattering centers. This model is supported by

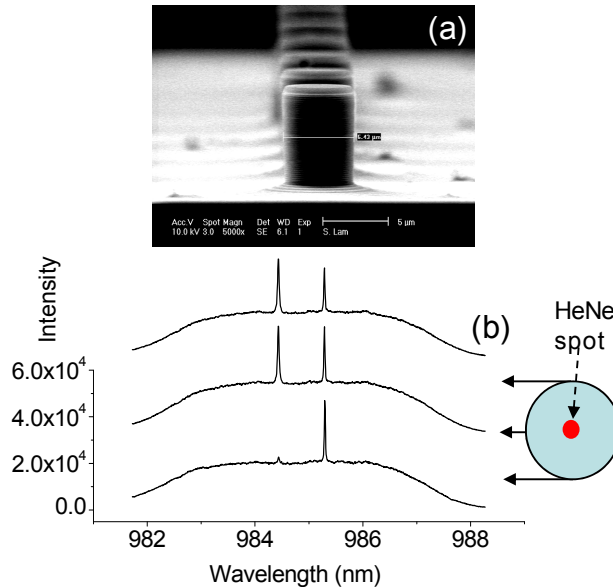


Fig. 3. (a) SEM image of 5.43 μm diameter GaAs/AlGaAs micropillars, (b) Split WGMs from 20 μm diameter pillar pumped by a HeNe laser.

numerical simulations performed by COMSOL software. It should be noted, however, that the fabrication of closely spaced semiconductor pillars required for efficient coupling between their WGMs turned out to be difficult. In addition, the problem of uncontrollable diameter variations cannot be solved in semiconductor structures. For these reasons, these structures were not used in our following studies of CROW structures.

4. Tapered Fiber-to-Microsphere Couplers

The next objective of the project was to establish controllable and reliable ways of coupling light in and out of microsphere-resonator circuits. FL properties of spheres cannot be used for developing device applications. To this end, we developed the apparatus based on using tapered fibers,³⁴ as illustrated in Fig. 4.

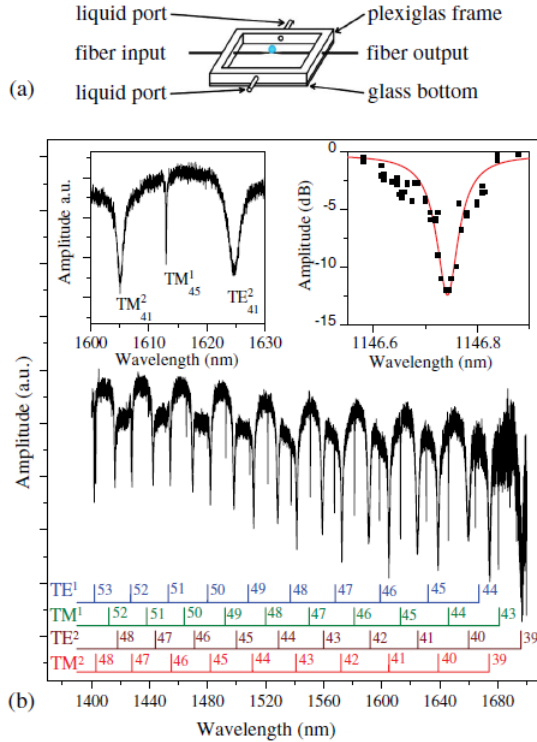


Fig. 4. (a) Sketch of the sample cell. (b) Transmission of the $d=2.5 \mu\text{m}$ fiber in contact with a BTG sphere with $D=14 \mu\text{m}$ and $n=1.9$ in water. Diagram marks calculated WGM peaks.

Our main interest was focused on using high-index microspheres ($n>1.8$) because such spheres have sufficiently large index contrast with water. As a result, they can be sorted or manipulated in water and they can be sufficiently small. We showed that high index ($n=1.9$ and 2.1) barium titanate glass (BTG) microspheres are perfect candidates for these applications due to their high- Q ($\sim 10^4$ in the $1100\text{--}1600 \text{ nm}$ range) resonances evanescently excited in spheres with diameters of $4\text{--}15 \mu\text{m}$, as illustrated in Fig. 4. By reattaching the spheres at different positions along a tapered optical fiber, we showed that the coupling constant exponentially increases with thinner fiber diameters. We demonstrate the close to critical coupling regime with intrinsic $Q=3 \times 10^4$ for water immersed $14 \mu\text{m}$ BTG spheres.

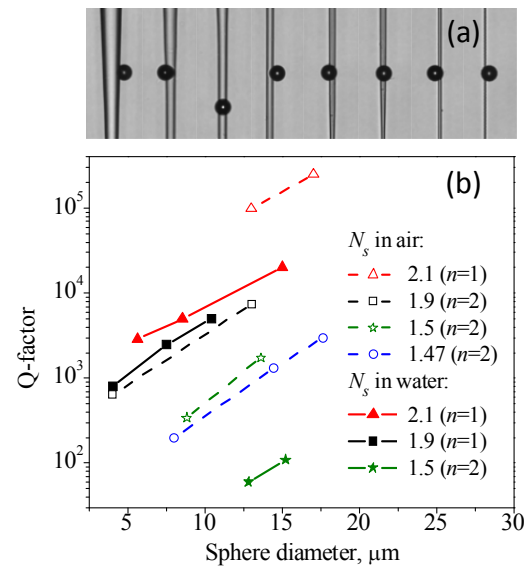


Fig. 5. (a) Tapered fiber-to-microsphere couplers with a sphere attached at different positions along the taper and (b) Q factors of WGMs in spheres with different index measured in air and water.

5. Observation and Study of Resonant Light Forces

The effect of resonant enhancement of light pressure exerted on microdroplets was observed by almost four decades ago by Arthur Ashkin and Joseph Dziedzic.³⁵ The effect has been weakly pronounced (small peak-to-background ratio for the optical force) because the incident light beam was not coupled to WGMs in droplets evanescently. It was probably one of the reasons why this pioneering paper has not been followed by a large number of publications.

In our work, we exerted the optical pressure on microspheres evanescently.^{36,37,38} We did it using tapered microfibers etched down to $\sim 1\mu\text{m}$ diameters. Such microfibers carry the optical power mainly outside the core. We developed special microfluidic platforms where such tapered microfibers can be permanently fixed and where the flux of a liquid suspension of microsphere can be provided perpendicular to the tapered microfiber or in any desirable direction.

It is well known that the radiative force exerted on totally absorbing particles are equal to P/c , where P is the incident optical power and c is the velocity of light. This is a fundamental limit of the radiative pressure determined by the total momentum flux carried by light. In the precise backward reflection case, in the case of mirror-like particles, the radiative force can reach the value of $2P/c$ which constitutes the absolute limit of the light forces.

Usually, in the case of optical manipulation with dielectric particles the forces are much smaller than these theoretical limits. This is determined by the fact that these dielectric particles are practically not absorbing light and by the fact that they scatter only few percent of the incident power and they scatter light in all directions in space. As a result, the conventional non-resonant momentum transfer from light to particles is inefficient. It can be less than $\sim 1\%$ of the total momentum flux or even smaller depending on the size and index of the particle and other parameters of the system. This situation routinely takes place in conventional optical tweezers.

In our work, we observed for the first time that the light forces exerted on dielectric microspheres under resonance with their WGMs can reach the total absorption limit. In addition, and this is very important property for developing applications of this technology, the peak-to-background values can have extraordinary high values. In fact, away from the resonance with WGMs the spheres cannot be even attracted to the tapered fiber because they are a subject for a Brownian motion, and the optical gradient force is not sufficiently strong to retain the spheres near the fiber taper. Such strongly pronounced resonant nature of the optical propulsion effects opens new ways of sorting microspheres by using light. The idea is that the microspheres

resonant with the frequency of the laser can be easily separated from the rest of the spheres and moved to a separate location. This opens totally new way of sorting dielectric microspheres with the accuracy determined by the Q-factors of their WGMs.

Initially, we discovered this effect of giant resonant light pressure in 2012-2013 by working with size-disordered assemblies of dielectric microspheres. The commercial suspensions of dielectric microspheres have $\sim 1\%$ diameter variations which translate into variations of the positions of the WGM resonances by several nanometers in different spheres. By studying statistical properties of propulsion of such spheres across tapered microfiber, we observed that a small fraction of such spheres (few percent) is optically trapped by the microfiber and propelled along the taper with extraordinary high velocity which exceeds previously observed velocities by more than an order of magnitude. We interpreted this effect as occurring due to a resonance between the wavelength of the laser and the wavelength of WGM in a given microsphere.

Our work was recognized as one of the major breakthrough results in optics and photonics in 2013 when it was included in the December Issue of the Optics and Photonics News. We published our observations in Nature/Light: Science and Application article in 2013.

During the period of extension of our ARO grant we further developed our experimental setup and observed this effect in refined conditions when we were able to control the detuning between the laser and WGMs individually for each sphere.³⁹ First, we integrated our fiber-integrated microfluidic platform with the optical tweezers that gave us a full positional control of individual microspheres and enabled a spectroscopic characterization of the WGM resonances prior to their propulsion. After that, as illustrated in Fig. 6, we realized spectrally resolved optical propulsion of microspheres with known amount of the detuning between the laser emission line and WGMs in microspheres. This allowed us to measure the spectral shape of the propulsion peaks by using measurements on multiple spheres with different detuning. We demonstrated that the spectral shape of the propulsion peak replicates (with an inverted shape) the spectral positions and shape of the dip in the fiber transmission spectra. As shown in Fig. 7, we also demonstrated that the magnitude of the optical propulsion forces effectively reaches the total absorption limit of the light momentum flux, P/c . We also showed that in the course of propulsion the microspheres are separated from the tapered fiber by a steady-state liquid gap. The stability of the radial trap was achieved due to a combination of the optical attraction at longer distances and electrostatic repulsion at the shorter distances from the fiber.

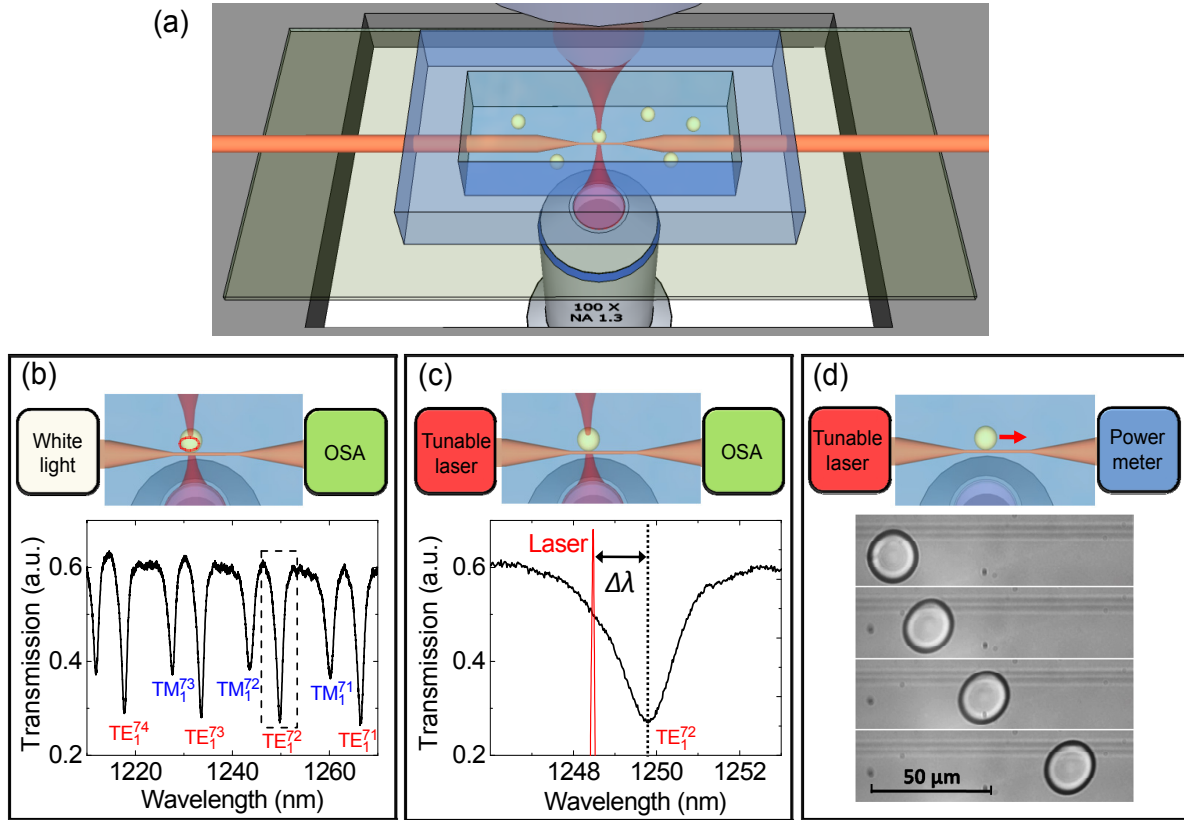


Fig. 6. (a) Overview of the tapered fiber coupler illustrating the manipulation of microspheres by the optical tweezers. (b-d) The sequence of experimental procedures: (b) Characterization of WGMs in a given sphere by fiber-transmission spectroscopy, (c) Setting the detuning of the laser emission line (narrow peak), $\Delta\lambda$, from the center of the dip in transmission spectrum, (d) Propelling of the 20 μm sphere along the tapered fiber represented by the snapshots taken with 100 ms time intervals.

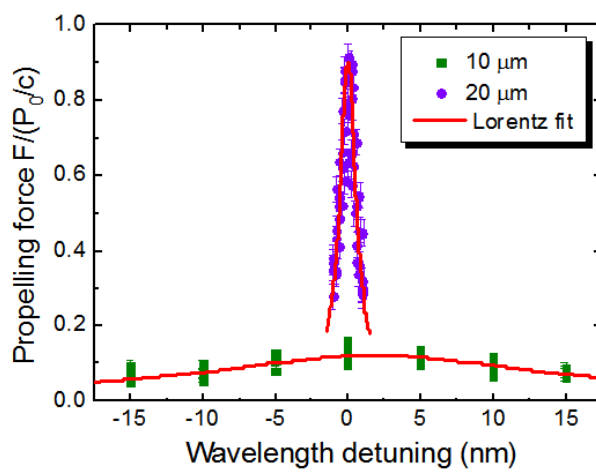


Fig. 7. Comparison of optical propelling force for 10 μm and 20 μm spheres as a function of the laser wavelength detuning from the WGM resonance.

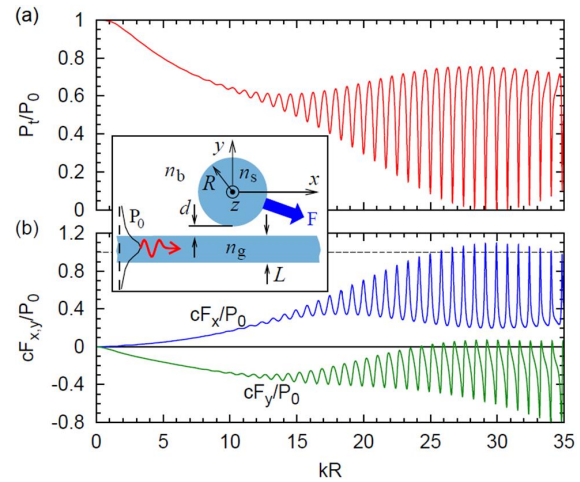


Fig. 8. (a) Transmitted guided power P_t/P_0 , (b) longitudinal, cF_x/P_0 , and transverse, cF_y/P_0 , forces as functions of the particle size parameter kR . The inset illustrates the geometry of 2-D model.

We developed a numerical modeling of the optical forces exerted on microspheres using a simplified 2D model. As illustrated in the inset to Fig. 8, the light was launched using a surface wave at the metallic boundary or a surface dielectric waveguide. The transmission spectra and the directionality of the scattered light were calculated by numerically solving Maxwell's equations. This made possible calculations of the spectra of optical forces, as illustrated in Fig. 8, which were found to be in a very good agreement with the experimental results.

One of the limitations of this work is related to the choice of material of the spheres which has to be polystyrene because for liquid propulsion it is required that the density of spheres should be sufficiently close to the density of the liquid. However, the refractive index contrast of polystyrene with water (1.59/1.33) was not sufficiently high that resulted in large diameters of polystyrene spheres ($D > 15 \mu\text{m}$) required for the experimental studies of resonant optical propulsion effects.

In order to overcome this limitation, we developed a theory of light forces exerted on microspheres by a beam focused in a vacuum, air or liquid environment.⁴⁰ It is shown that a focused beam produces forces that depend strongly on the detuning between WGMs and laser frequencies. Such forces lead to the enhancement of the longitudinal (along the beam) velocities for the resonant particles as they exit the beam. The sorting can be performed in vacuum or in viscous media resulting in different spatial separation of the particles. We show that this is an enabling technology for sorting of resonant microspheres with better than 0.01% uniformity of WGM peaks. It is particularly important that this method is applicable to high-index spheres, such as $n \sim 1.9$, which can possess $Q \sim 10^4$ in sufficiently small particles, $D \sim 3 \mu\text{m}$, suitable for developing chip-scale structures and devices.

These studies showed that sufficiently large resonant optical forces can be exerted on microspheres each time they traverse the waist of the focused laser beam. The force difference between resonant and non-resonant cases was found to be easily detectable, if, as an example, the microspheres were allowed to continue free falling motion in vacuum or air environment after traversing the laser beam. This theory allowed us to calculate the trajectory of the microspheres during and after their interaction with the focused laser beam and suggest techniques of sorting the spheres by using light which would be applicable to high-index spheres which usually have density much higher than the density of water.

6. Spectral Fingerprints of Photonic Molecules

In the same way as chemical molecules have properties determined by the number and configuration of the constituting atoms, the similar properties are expected for photonic molecules. Of course, there are some important differences. In quantum mechanics, the atoms are indistinguishable, whereas in classical mechanics this is not the case. Due to the size and shape variation the photonic atoms have varying energy positions of their WGM resonances. However, almost identical atoms can be selected using the technologies proposed in this project. Most importantly, even in resonant case, the electromagnetic coupling between photonic atoms is fundamentally different from the electronic hybridization effects taking place in real atoms. However, some element of analogy persists, and in order to prove that we performed modeling presented in Fig. 9.

The fiber transmission spectra show that depending on total number of atoms and their spatial arrangement, there exists a reproducible pattern of resonances which is representative of a given molecule and can even be used for its identification. It is seen that if the index or size of atoms is varying, the appearance of spectral features and the amount of splitting can change, but the overall appearance remains to be self-similar. We termed this property “spectral signature” of photonic molecule. Roughly speaking, each photonic molecule can be represented by the number of the split WGM components (which can be equal or less than the total number of spheres) and by the amount of their splitting relative to the position of uncoupled resonance. In the right column of Fig. 9, we presented spectral signatures of the molecules illustrated in the left column of this figure.

Obviously, each split component represents a particular spatial configuration of coupled WGMs excited in a given molecules, as illustrated in Fig. 10. They show a future prospect of photonic molecule engineering, since any desirable spectral shape can be achieved by manipulation with the microspheres. Such capability is rather unusual because in the case of standard in-plane fabrication technology (coupled microrings or disks) the individual atoms are fixed on the substrate. In contrast, in the proposed microspherical photonics, the atoms are easily movable and reconfigurable that opens a possibility for building spectral filters, delay lines and spectral sensors with desired characteristics.

In order to provide a demonstration for the proposed technology, we sorted polystyrene microspheres with diameters around 20 μm with almost identical positions of WGM peaks, and

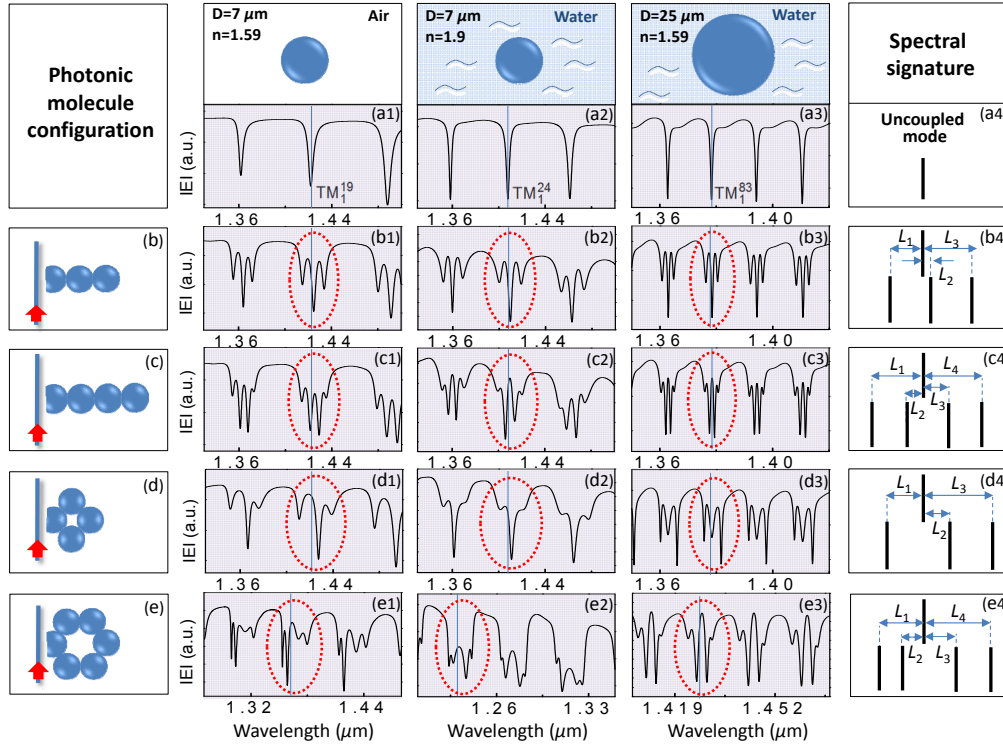


Fig. 9. Simulated transmission spectra of single resonators and various molecule configurations (b-e) with constituting atoms of (a1-e1) $7\ \mu\text{m}$ 1.59 index sphere in air, (a2-e2) $7\ \mu\text{m}$ 1.9 index sphere in water and (a3-e3) $25\ \mu\text{m}$ 1.59 index sphere in water, respectively. (a4-e4) Summarized spectral signatures for corresponding photonic molecules.

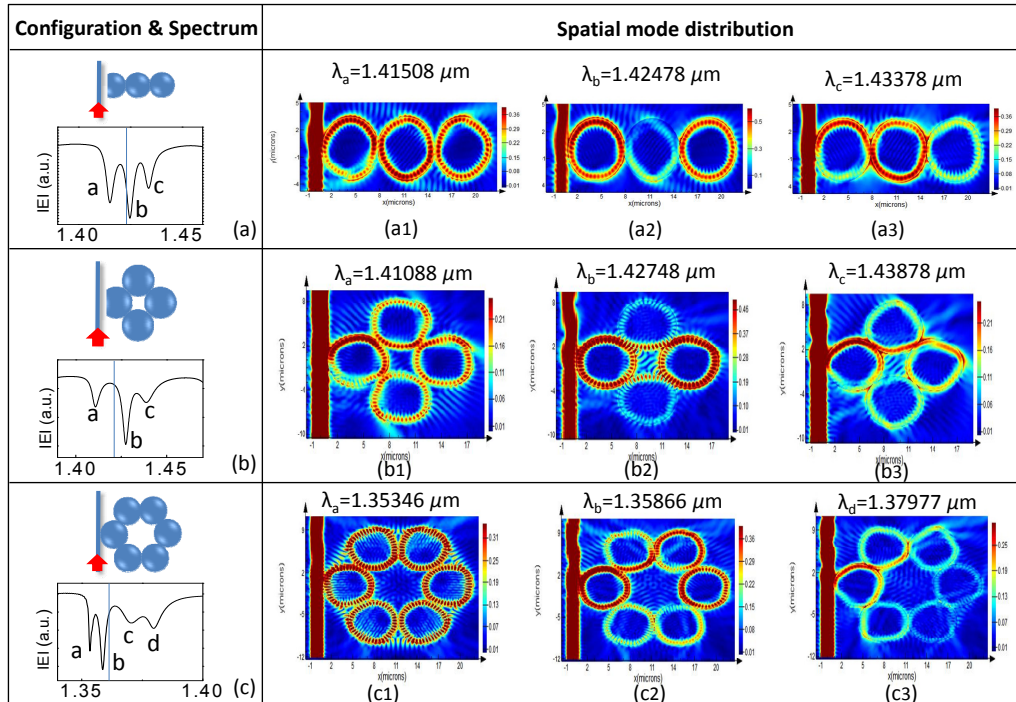


Fig. 10. Simulated EM field map at supermode eigen wavelengths for three different molecule configurations.

built various photonic molecules, as illustrated in Fig. 11. The characterization was performed using a tapered microfiber in contact with microspheres placed on substrate in such a way that the fiber was coupled to fundamental equatorial WGMs in spheres. The spectroscopic characterization was performed using our equipment obtained using our ARO DURIP grants. The characterization was performed in a water environment since it somewhat simplified these experiments. However, this is not a principle limitation for this technology and similar studies can be also performed in air. Water environment can be useful for sensor applications, whereas the air environment provides higher refractive index contrast for spheres which can be used for developing more compact structures. Another resource for achieving compact photonic

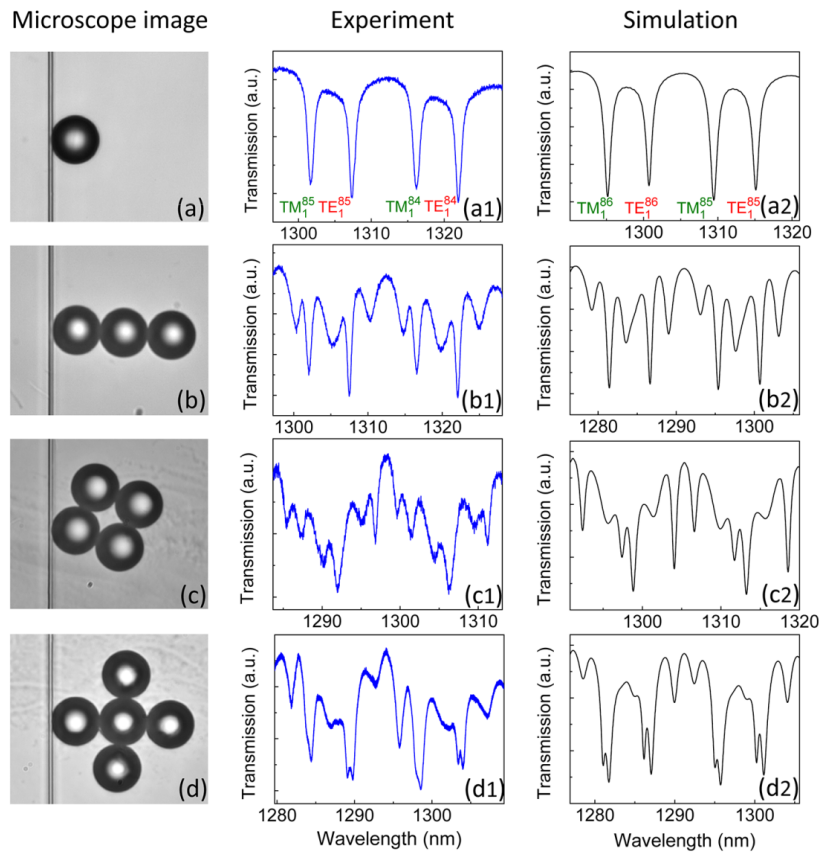


Fig. 11. (a-d) Microscope images for various photonic molecules assembled with size-matched polystyrene microspheres of 25 μm mean diameter side-coupled to a tapered fiber with 1.5 μm waist diameter in water. (a1-d1) Measured and (a2-d2) simulated fiber transmission spectra for corresponding molecule configurations.

molecules is based on using high-index spheres with $n > 2$. To identify the spectral signatures, we performed finite different time domain modeling of the fiber transmission spectra using a simplified 2D model, but with all parameters matching our experimental situation in the equatorial plane of microspheres. The comparison of the experiment and theory in Fig. 11 demonstrate their agreement that provides strong support for the WGM coupling models proposed and realized in this work.

7. Microsphere-Chain Waveguides

This Section of the report is devoted to fundamental studies of mechanisms of the optical transport and focusing properties of periodical chains of dielectric microspheres. In recent years the microsphere-chain waveguides (MCWs) emerged as a paradigm for photonic applications.⁴¹ Historically, the interest was focused on coupling between WGMs in spheres,¹⁹⁻²³ however, gradually, it moved to studies of periodical relaying effects.⁴²⁻⁴⁷ It was demonstrated that the optical mode of such structures has a period equal to the size of two spheres ($2D$).^{27,28} Initially, these modes have been observed²⁷ in mesoscale MCWs formed by the spheres with $D < 10\lambda$. They have been termed nanojet-induced modes (NIMs)²⁷ based on analogy with tightly focused beams, “photonic nanojets”, produced by individual spheres.

In this ARO project, we initially studied the transport and focusing properties of such chains in the limit of geometrical optics.⁴⁸ In this limit, we termed these modes “periodically focused modes” (PFMs). We showed that a particularly interesting PFM’s property is their minimal propagation losses, which is achieved due to Brewster angle conditions periodically reproduced along the chain for radially polarized beams.^{48,49} We also demonstrated that if a multimodal source is used for illumination, many modes can be coupled to MCW, however, only PFMs would survive in sufficiently long chains. It has been observed that this process leads to formation of progressively smaller focused beam waists along the chain. It has been demonstrated that in the geometrical optics limit such “beam tapering” effect takes place in a relatively narrow range of indices $1.72 < n < 1.85$.^{48,49}

In Section 7.1 we will mainly concentrate on experimental results of studies of MCWs where we realized⁵⁰ a gradual step-by-step transition from geometrical (ray optics) to mesoscale (wave optics) case by decreasing the mean diameters of the spheres comprising MCWs from $\sim 60\lambda$ to $\sim 4\lambda$. We showed that the beam tapering effect (gradual reduction of the focused beam waists) is absent for spheres with $D \geq 20\lambda$, as expected from geometrical optics. However, we found that this effect is extremely well pronounced for spheres with $D \leq 10\lambda$. The observed effects are found to be in a qualitative agreement with a full-wave numerical modeling. We also demonstrate that the propagation losses in mesoscale chains are too small (~ 0.1 dB/sphere) to be explained by geometrical optics. We will describe polarization properties of MCWs using geometrical optics in Section 7.2. We will consider laser-scalpel applications of MCWs in Section 7.3.

7.1 Transport and focusing properties

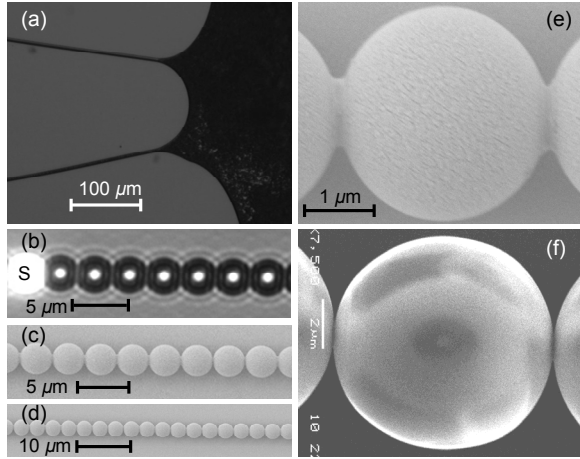


Fig. 12. (a) Image of the self-assembly process. (b) Optical and (c), (d) SEM images of MCW formed by $3\mu\text{m}$ spheres. (e), (f) SEM images of micro-joints between spheres with $D=3$ and $10\mu\text{m}$, respectively.

Chains of undoped polystyrene spheres (Thermo Fisher Sci.) with D varying from 30 to $2\mu\text{m}$ were self-assembled on glass substrates.⁵⁰ In this method the liquid film with spheres is sandwiched between two hydrophilic microscope slides. The evaporating liquid microflows stretch from massive deposits of microspheres to “pinning” points nucleated by bigger spheres or by the defects on the substrate, as shown in Fig. 12(a). Evaporation of microflows in a lateral direction leads to the formation of straight and long chains of touching spheres illustrated in Figs. 12(b-d).

The structures were characterized with an inverted IX-71 Olympus microscope. Fluorescent (FL) dye-doped, size-matched polystyrene spheres were used as local light sources (S-sphere) for each chain.

The beam tapering effect is illustrated in Fig. 13(a,b) for MCWs formed by $5\mu\text{m}$ spheres. It is seen that the waists of the beams intersecting the contact regions between the spheres becomes narrower, if the sphere diameters are smaller or equal to $5\mu\text{m}$.

To accurately compare the results of the optical transport and focusing properties in MCWs with drastically varying sizes from 30 to $2\mu\text{m}$, it is essential to present the results in dimensionless units, as shown in Fig. 13. The FWHM measured after N^{th} sphere was normalized by the FWHM after the first sphere, Y_N/Y_1 . Due to multimodal nature of the S-sphere emission, we typically observe a broad beam after the first sphere, $Y_1 \sim D/3 - D/2$. As seen in Fig. 13(b), MCWs comprised of spheres with $D/\lambda \geq 20$ ($D \geq 10\mu\text{m}$) do not demonstrate a pronounced beam tapering effect. However, the mesoscale MCWs comprised of spheres with $4 \leq D/\lambda \leq 10$ ($2 \leq D \leq 5\mu\text{m}$) demonstrate a significant FWHM reduction with $Y_{10}/Y_1 < 0.4$. For MCWs formed by smallest spheres, $D=2$ and $3\mu\text{m}$, it takes approximately 10 spheres for FWHM to reach the dimensions $Y_{10} \sim 0.4 - 0.5\mu\text{m}$ determined by the diffraction limit of our imaging system.

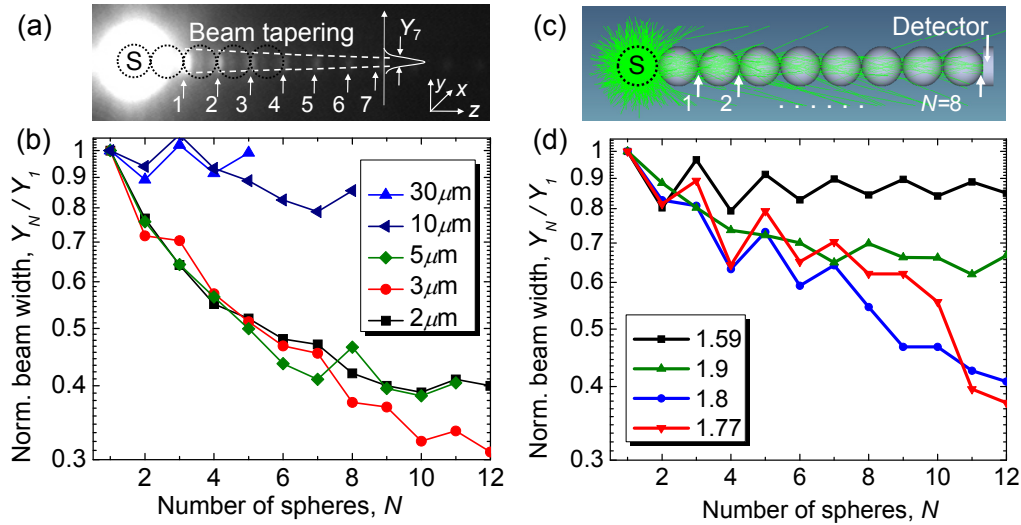


Fig.13. (a) Optical image of MCW showing the near contact regions where the beam profiling was performed, (b) Experimental results of the beam profiling at different distances from the source (S) sphere for spheres from 2 to 30 μm in diameter, (c) Illustration of numerical ray tracing performed to study the evolution of the beam profile through MCW. (d) Beam widths determined using geometrical optics.

The MCWs beam tapering properties were modeled using ZEMAX-EE ray tracing software, as illustrated in Fig. 13(c). Chains of N identical spheres with $n=1.59$, 1.77, 1.8, and 1.9 were studied. The emission of dye-doped sphere was modeled by using point ray sources with random polarization distributed inside S-sphere.

The evolution of the spatial beam profile was investigated at the interface between spheres using a flat square detector with the size equal to D . Intensity distributions were calculated from the density of rays at the detector plane. It can be seen from Fig. 13(d) that MCWs comprised of spheres with $n=1.77$ and 1.80 demonstrate marked FWHM reduction ($Y_{12}/Y_1 \sim 0.4$). This beam tapering effect is attributed to gradual filtering of periodically focused modes (PFMs) in such structures. Significantly smaller beam tapering ($Y_{12}/Y_1 \sim 0.7$) was observed for $n=1.9$. For our experimental case of $n=1.59$, such effect was practically absent, consistent with our measurements for spheres with $D/\lambda \geq 20$ ($D \geq 10 \mu\text{m}$).

In order to shed some light into properties of mesoscale MCWs, we performed full wave modeling by finite element method (FEM) illustrated in Fig. 14. The simulation was performed using COMSOL Multiphysics in 2D case for a chain of touching, lossless, dielectric cylinders with diameters of $5 \mu\text{m}$ and index 1.6. As a light source, we used an S-cylinder containing 1400 dipole emitters at $\lambda = 0.53 \mu\text{m}$ schematically shown in Fig. 14(b). The dipoles with various oscillation directions were randomly placed along several radial lines inside the S-cylinder.

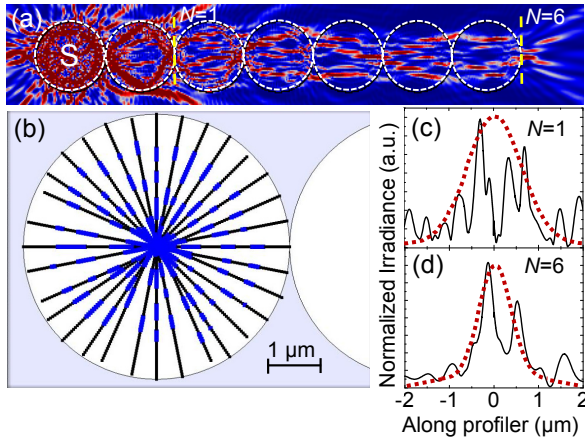


Fig. 14. (a) 2D irradiance map obtained by the FEM simulation for an MCW. (b) Model of S-cylinder with dipoles placed along radial directions with different oscillation directions. Irradiance profiles after (c) the first and (d) the sixth cylinder illustrating the beam tapering effect (red dashed curves).

The results presented in Fig. 14 are generally consistent with the beam narrowing effect. After the light has propagated through six cylinders a large fraction of the modes is leaked out of the cylinder-chain waveguide, resulting in a narrower beam waist with $Y_6 \sim 1 \mu\text{m}$, as illustrated by the envelope in Fig. 14(d). However, the calculated irradiance profiles also show a complicated multimodal nature of propagating beams due to coherent nature of the source. This modeling shows that in mesoscale MCWs these effects take place at smaller indices (~ 1.6) compared to

the geometrical optics case.

Gradual filtering of extremely low-loss NIMs in such chains can be a key factor for the explanation of the MCWs attenuation properties presented in Fig. 15. As illustrated in Fig. 15(b), for a distant section of the chain with $35 \leq N \leq 39$ the measured losses are found to be 0.076, 0.12, and 0.15 dB/sphere for $2 \mu\text{m}$ (red star), $3 \mu\text{m}$ (magenta square), and $5 \mu\text{m}$ (blue triangle) spheres, respectively.

These losses are far below than any estimation based on geometrical optics.⁴⁸ The geometrical optics modeling of attenuation per sphere with the spherical source for the same section of the chain ($35 \leq N \leq 39$) is represented by the curve in Fig. 15(b). The geometrical optics predicts a local minimum of attenuation ($\sim 0.2 \text{ dB/sphere}$) in a narrow range of indices around $n=1.77$ due to filtering of PFMs with the $2D$ period and radial state of polarization. For the experimentally studied case of $n=1.59$ the geometrical optics predicts attenuation $\sim 0.4 \text{ dB/sphere}$.

As it can be seen in Fig. 15(b), the experimentally observed attenuation in such chains is significantly smaller than the smallest values of attenuation predicted by geometrical optics at any n from 1.4 to 2.4 (for $35 \leq N \leq 39$).

The explanation of such small losses can be related to the fact that in the limiting transition to small spheres, $D \ll \lambda$, MCW can behave almost like a single-mode low-loss

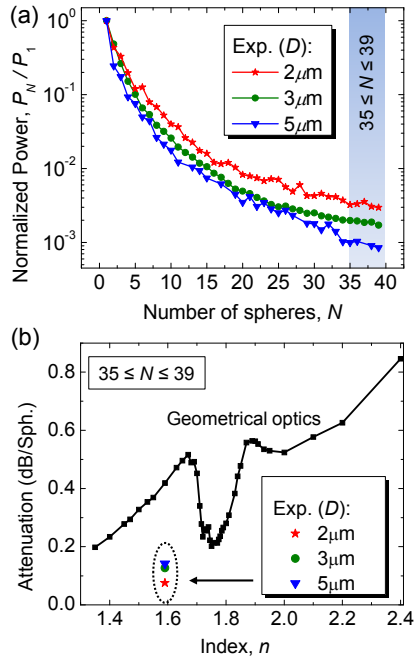


Fig. 15. (a) Normalized power loss measured in MCWs formed by the polystyrene microspheres with $D=2, 3$, and $5\mu\text{m}$. (b) A comparison with the geometrical optics model.

nanofiber with effective index guiding, where losses per nanosphere can be extremely small.⁵¹ An additional factor which can play an important role in our experiments can be connected with microjoints⁴⁴ inevitably occurring between the polystyrene spheres. Such microjoints can significantly reduce scattering losses in periodically relaying structures.

In conclusion, it was demonstrated that mesoscale ($4 \leq D/\lambda \leq 10$) self-assembled polystyrene sphere-chain waveguides, coupled to a multimodal source, gradually filter periodically focused beams with the diffraction-limited beam waists. We showed that such “beam tapering” takes place at much smaller indices ($n=1.59$) than it is predicted by geometrical optics. The propagation losses deeply inside such chains were also found to be smaller than any prediction based

on geometrical optics. The results of this work are important for developing waveguiding structures with focusing capability which can be used as local microprobes, ultraprecise laser scalpels, and polarization filters,^{52,53} considered in the next Section.

7.2 Polarization properties

The polarization effect introduced by a chain of spheres stems from the fact in geometrical optics the rays with a particular axial offset, $r/D=\sqrt{3}/4$, and TM polarization can propagate with extremely small losses for spheres with refractive index $n=\sqrt{3}$.⁴⁸ This is a simple consequence of the Brewster’s law, it is interesting, however, to consider different spheres’ indices and study if PFMs can still exist under these conditions. The idea of our analysis is that in order to remain $2D$ periodic, such modes should have different off-axial shifts. Their external (θ_i) and internal (θ_r) angles of incidence and refraction, respectively, would not be exactly equal to those following Brewster’s law, but they can be sufficiently close to the optimal values. Most importantly, these angles would be periodically reproduced as light propagates through the chains which would help to keep the losses low.

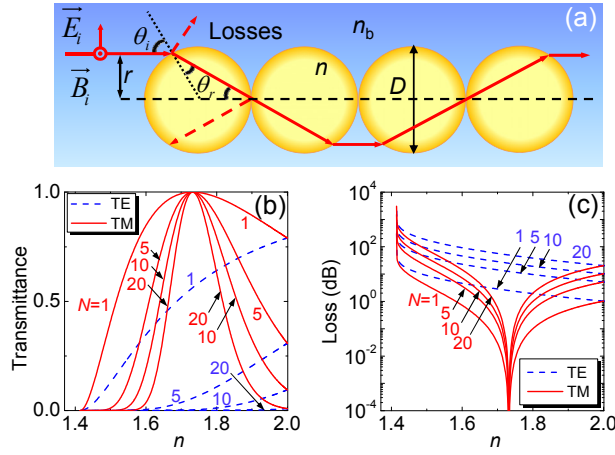


Fig. 16. (a) Ray tracing of PFM with 2D period. (b) Transmittance and (c) loss in chains of $N=1, 5, 10$ and 20 spheres as a function of n for TE and TM polarizations of the incident ray

account Fresnel reflection coefficients⁵⁴ at each spherical interface from the following equations for TE and TM polarizations:

$$R_{TE} = \frac{\sin^2(\theta_i/2)}{\sin^2(3\theta_i/2)}, \quad (1)$$

$$R_{TM} = \frac{\tan^2(\theta_i/2)}{\tan^2(3\theta_i/2)}, \quad (2)$$

The transmittance and corresponding reflection losses for rays with TE and TM polarizations as a function of n for chains of $N=1, 5, 10$ and 20 spheres are presented in Figs. 16(b) and 16(c), respectively. It is illustrated in Fig. 16(c) that for 10-sphere long chains with $1.68 < n < 1.80$, TM polarized PFM have total propagation losses smaller than 1 dB, i.e. less than 0.1 dB/sphere. Conversely, for TE polarization the total PFM losses exceed 20 dB in the same range of indices. This means that for randomly polarized collimated incident rays, the output has mainly TM polarization component. Due to axial symmetry of the problem, the global state of polarization (SOP) of the transmitted beam should be increasingly radial.

The DOP $P(\mathbf{r})$ is defined as the ratio of the (averaged) intensity of the polarized portion of the beam to its total (averaged) intensity, both taken at the same point⁵⁵. This rigorous and unambiguous definition of the DOP is, however, sometimes difficult to use in practical cases. In such situations various *ad hoc* definitions of the DOP are frequently used in the form:

The attenuation properties of chains of spheres were studied by considering rays forming configurations with 2D period. For each index it was achieved by adjusting θ_i and r according to the following equations: $\theta_i = 2 \cos^{-1}(n/2n_b)$, $r/D = 0.5 \sin(\theta_i)$, where $n_b=1$ is the refractive index of the background medium. Based on these equations, it can be deduced that quasi-PFMs exist in a broad range ($\sqrt{2} < n < 2$) of indices. Propagation losses for the incident rays illustrated in Fig. 2(a) can be estimated by taking into

$$Q(r) = \frac{|I_x(r) - I_y(r)|}{I_x(r) + I_y(r)}, \quad (3)$$

where I_x and I_y are the averaged intensities in two mutually orthogonal directions, their choice being suggested by the geometry of the problem. Unlike the $P(\mathbf{r})$, the quantity $Q(\mathbf{r})$ depends on the choice of the x, y axes. It has been theoretically demonstrated, however, that the *ad hoc* definition in the form of Eq. (3) will correctly represent the degree of polarization $P(\mathbf{r})$, provided that I_x and I_y are taken to be true eigenvalues of the polarization matrix representing the symmetry of a given problem.⁵⁵ The axial symmetry of the chains of spheres implies that their polarization eigenvalues should be represented by the intensities of radially (I_r) and azimuthally (I_ϕ) polarized beams.

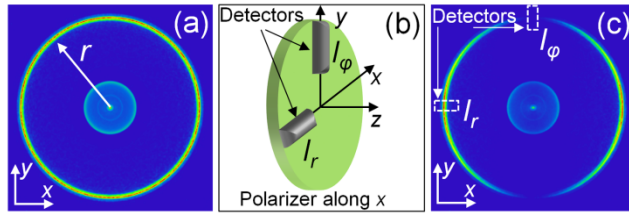


Fig. 17. (a) Intensity distribution produced by 20-sphere long chain with $n=\sqrt{3}$ as a result of illumination with collimated rays. (b) Linear polarizer (along x) placed after the end-sphere and the detectors. (c) Intensity distribution with the polarizer installed also showing positions of two detectors (dashed rectangles) used for DOP calculations.

Typical intensity distribution calculated for spheres with $n=\sqrt{3}$ using a flat detector in contact with the end sphere is illustrated in Fig. 17(a) in the case of collimated incident rays for 20-sphere long chain. This case is representative of the calculations performed for chains formed by even number of spheres with $n=1.65-1.85$. For this range of indices the output beams consist of: i) A ring with radius r determined by the

PFM axial offset, ii) central beam formed by paraxial rays, and iii) A weak background illumination. The dominant contribution to the output optical power is given by the ring with radius r .

In order to estimate the DOP, we placed a horizontally oriented linear polarizer (along x) after the end-sphere, as shown in Fig. 17(b). The azimuthal intensity modulation along the ring in Fig. 17(c) carries information about DOP of the transmitted beam. Using different positions of the detector indicated in Fig. 17(c) and using relationships $I_x=I_r$ and $I_y=I_\phi$ in Eq.(3), we calculated the degree of radial polarization as a function of n for chains with different lengths. We ensured good convergence of the results with reduction of the width of the detectors. Numerical modeling was performed by using ZEMAX-EE.

In Fig. 18 the results of calculations of DOPs are presented for three types of ray sources: collimated incident rays (Fig. 18(a)), spherical emitter (Fig. 18(b)), and multimode fiber (Fig. 18(c)). It is seen that DOP increases with the length of the chain reaching ~ 0.9 for 10-sphere chains with $1.68 < n < 1.80$. The highest DOP can be obtained for collimated input beams, as shown in Fig. 18(a).

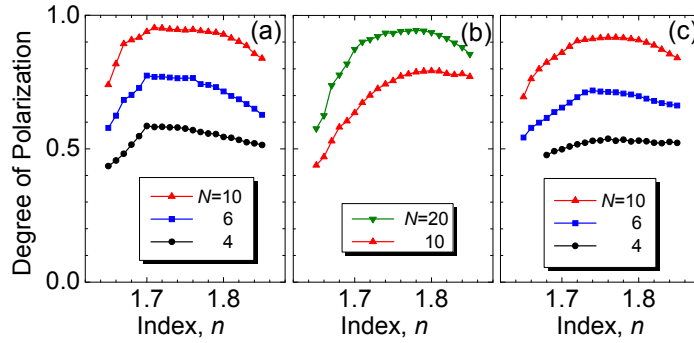


Fig. 18. (a-c) Degree of radial polarization versus n calculated for three types of ray sources illustrated in Figs. 21(a-c), respectively.

In conclusion, we showed that the chains of spheres filter radially polarized beams. The optimal refractive index for observation of these effects is very close to the index of one of the best quality infrared materials, sapphire (or ruby) with $n \approx 1.71$, which means that various practical IR focusing and polarization devices can be built using sapphire cylinders or spheres. In addition, since focusing of radially polarized beams can be sharper than the focusing of unpolarized or linearly polarized beams, such purely dielectric structures can be very useful in high resolution polarization imaging and in the design of various devices including focusing microprobes, laser scalpels, and optical tweezers.

7.3 Laser-surgery applications

In this section, we will provide a brief review of our results based on application of MCWs for developing ultra-precise multimodal microprobes for laser-tissue surgery. This work was performed in collaboration with a laser surgery expert from our department, Dr. Nathaniel Fried, and retinal surgeons, Drs. Howard Ying (Johns Hopkins University) and Andrew Antozsyak (Charlotte Eye, Nose & Throat Associates). Our contribution to this work is based on a proposal of using a chain of dielectric microspheres for focusing multimodal laser beam under contact with tissue.⁵⁶⁻⁵⁹

Conventional fiber-optic-based surgical laser probes are designed to operate either at a fixed working distance from the tissue or in contact with the tissue with relatively large spot diameters (e.g., $>100 \mu\text{m}$). These fibers and laser probes are not widely used in intraocular laser surgery, except for thermal coagulation, because they lose their ability to focus light in aqueous media. In contrast, the novel laser probe discussed here may operate to ablate the tissue in contact mode. The highly focused beam at the probe's surface combined with the short optical penetration depth of the erbium:YAG laser may allow better surgical results in more sensitive and thin areas like the macula, where detailed vision is achieved and surgical precision is most important. Replacement of mechanical intraocular surgical instruments with a laser probe that

has a much smoother tip with a tractionless method for tissue engagement may also reduce mechanical retinal surface damage as well as retinal detachments.

As a laser source, we selected the Er:YAG laser because the 2940-nm wavelength closely matches a major water absorption peak in tissue, resulting in an optical penetration depth (OPD) of approximately 5 to 10 μm for soft tissues. Over the past 20 years various optical devices including spheres, hemispheres, domes, cones, slanted shapes, cylindrical gradient index (GRIN) lenses, and tapered fibers have been used as tips for ophthalmic laser scalpels. However, these devices are typically designed to operate in noncontact mode in air at a fixed working distance from the tissue. Contact mode probes can be created by placing a single sphere with a high index of refraction, between 1.7 and 2.0, at the end of a waveguide or optical fiber. Spheres at these indices will focus an incident plane wave on the back surface to a focal point near the front surface. Fast focusing through the sphere also creates a fast divergence after the sphere. This property can be used to decrease the effective penetration depth in tissue by allowing only the light near the surface of the sphere to have an energy density sufficient to ablate tissue. Working

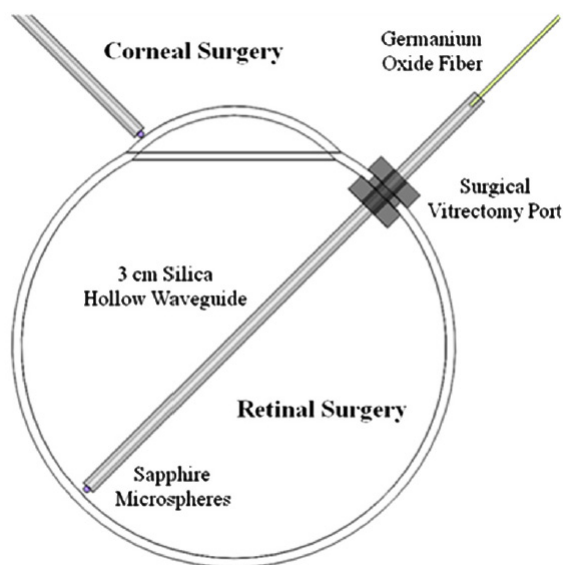


Fig. 19. Proposed ophthalmologic surgical configurations consisting of a 30-mm-long hollow waveguide of 0.75-mm diameter with microsphere focusing at distal tip. The diameter of a typical human eye is 24 mm.

in contact mode eliminates any intervening water layer which would otherwise strongly attenuate the mid-IR laser radiation. Recently, we showed that chains of microspheres in odd multiples at these indices reduce the spot size of the laser beam through filtering of nonperiodically focused modes (PFMs).^{48,49} The purpose of this study is to test a mid-IR laser and novel fiber optic probe for precise ablation of a thin layer of tissue, in contact mode, with minimal collateral thermal damage to underlying tissue, for potential application in ophthalmic surgeries.

Simulations of the multimode fiber output, hollow wave guide (HWG), and three

different sphere configurations were modeled using Zemax (Radiant Zemax LLC, Redmond, WA). Figure 20 shows the light source modeled as the germanium oxide fiber's 150- μm core

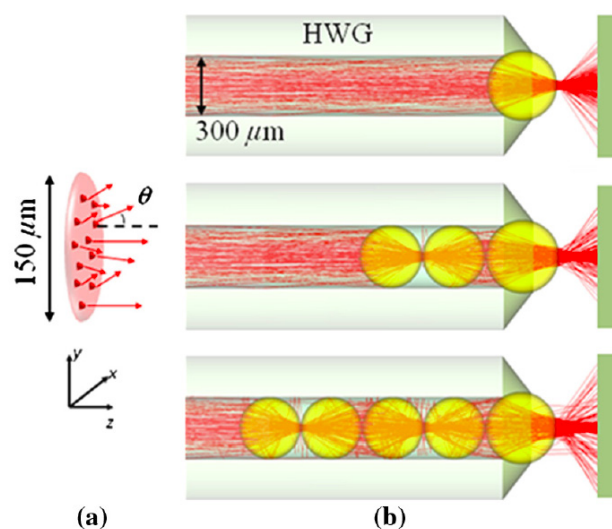


Fig. 20. (a) Source: representation of the 150-μm-core germanium oxide fiber tip, which is inserted into the proximal end of the 3-cm-long HWG. (b) Beam Shaping: one-, three-, and five-sphere configurations consisting of 300-μm and 350-μm spheres with refractive indices of 1.71.

with a full cone angle of 12 deg. For all presented simulations a total count of 20 million rays was used. At the distal tip three different $n=1.71$ sphere configurations were modeled in air, as shown in Fig. 20(b). The analysis plane was placed at the minimal beam waist beyond the end sphere.

Characterization of the probe's beam-shaping performance was conducted before tissue studies. One-, three-, and five-sphere structures were tested to determine their relationship to spot size and transmission. Figure 21(a) and the top row of Fig. 22 show the simulation results for intensity distribution at the minimum spot size after the end sphere,

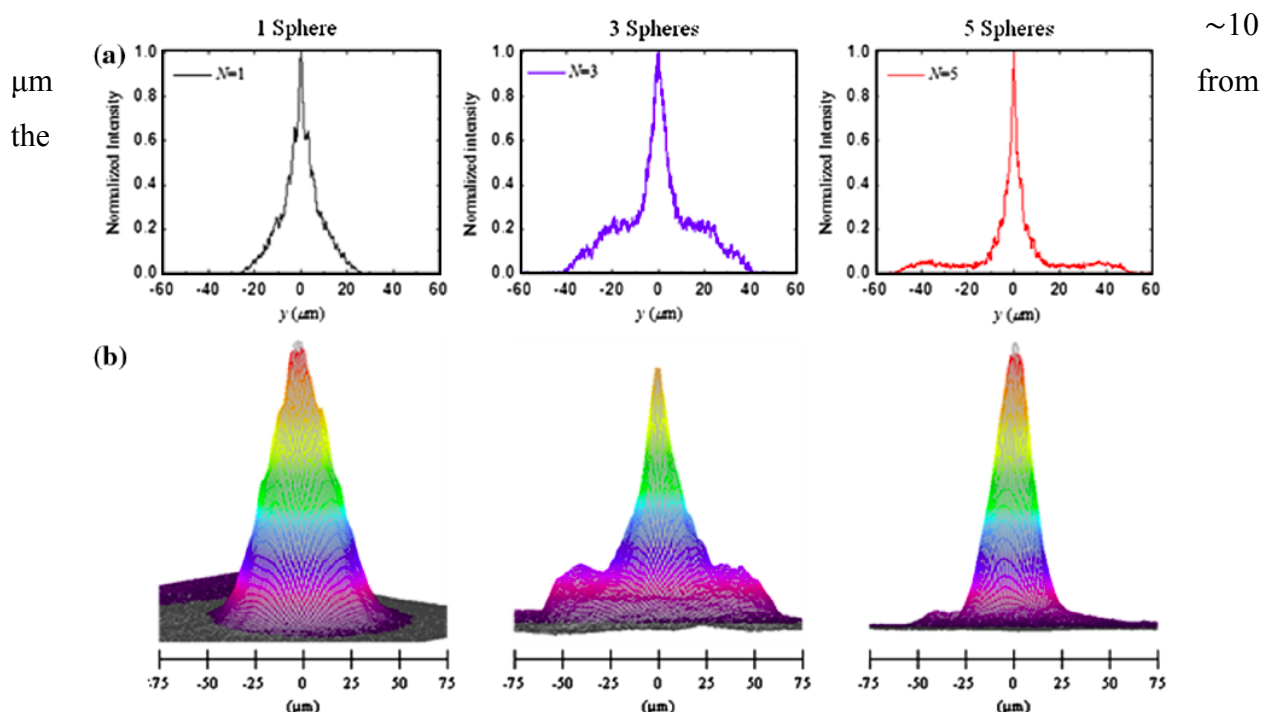


Fig. 21. (a) Normalized simulation of the intensity measured at the minimum beam waist (FWHM) for one-, three-, and five-sphere configurations. (b) Three-dimensional beam profiles acquired by magnifying the minimum beam waist onto the IR beam profiler's detector array. As the number of spheres increase, a reduction in FWHM spot diameter and an expanding low intensity mode-filtering ring can be seen in both simulation and experiment.

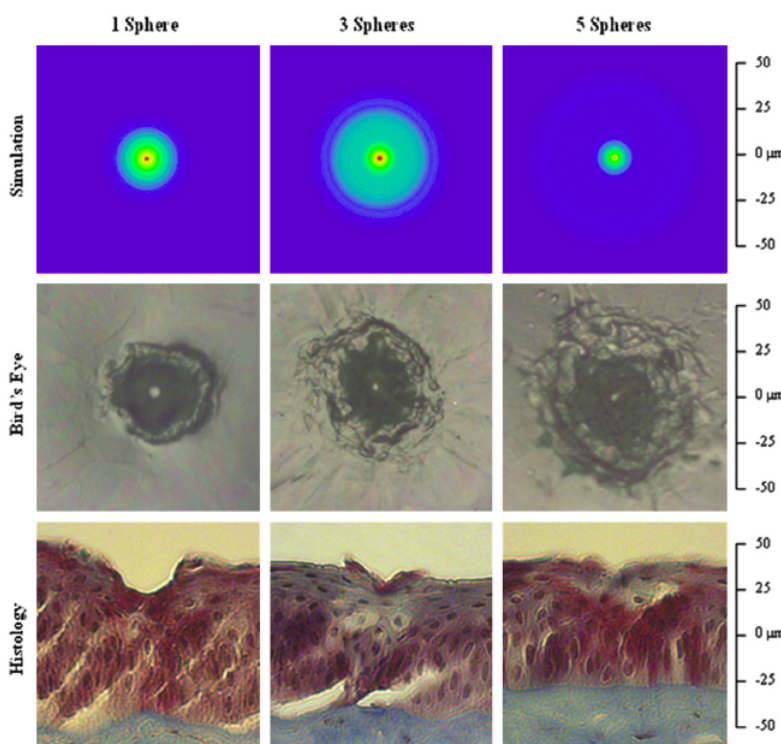


Fig. 22. (top row) Simulated intensity profiles for one-, three-, and five-sphere probes at minimum spot size occurring at $10\ \mu\text{m}$ after sphere vertex. (middle row) Representative bird's eye corneal crater images for one-, three-, and five-sphere probes at $0.1\ \text{mJ}$. (bottom row) Representative histology images for one-, three-, and five-sphere probe craters at $0.1\ \text{mJ}$ with trichrome stain.

vertex. The full width at half maximum (FWHM) measured from the simulation for each configuration of one, three, and five spheres is 8, 9, and $4\ \mu\text{m}$, respectively. The averaged FWHM beams measured for one, three, and five spheres were 67, 32, and $30\ \mu\text{m}$, respectively, with representative beam profiles shown in Fig. 21(b).

Various pulse energies between 0.02 and $1.0\ \text{mJ}$ at duration of $75\ \mu\text{s}$ were tested to experimentally determine the ablation threshold of the cornea. Since each sphere chain configuration (one, three, or five

spheres) attenuated the energy differently, attenuation of the laser output was adjusted to normalize each configuration to an incident energy of $0.1\ \text{mJ}$ on the tissue surface. Over 50 craters for each structure were measured, and the average crater widths are illustrated in Fig. 22.

In conclusion, a $750\text{-}\mu\text{m}$ -outer-diameter intraocular scalpel utilizing microsphere lenses was developed that is capable of delivering Er:YAG laser pulse energy to ocular tissue and creating ablation craters with widths between 15 and $50\ \mu\text{m}$ in contact mode. Different scalpel configurations with varying sphere chain lengths were successfully simulated and tested under ex vivo conditions on corneal tissue near the ablation threshold, demonstrating ablation crater size reduction for increasing number of microspheres, but with an increase in thermal damage. The small spatial beam size combined with the short optical penetration depth of less than $20\ \mu\text{m}$ could make this probe useful for precise contact ablation of exudates during surgery for PDR. Future studies will involve further development of the microsphere probe and in vivo studies in a PDR animal model.

8. Super-Resolution by Microspheres

The fundamental nature of the diffraction limit means that it forms an unavoidable barrier in any far-field imaging system. In addition, Abbe, Rayleigh, Sparrow, and Houston resolution criteria show that the limit of lateral resolution in such systems is about half the wavelength (λ). The objects of nanoscale science and technology (e.g., sub-cellular structures, viruses, proteins, and carbon nanotubes), with dimensions less than 100nm, therefore cannot be resolved with the use of a standard optical microscope. New physical principles (e.g., detection of optical near-fields or the use of strong non-linear effects) are thus needed to increase the resolution of imaging systems beyond the diffraction limit.⁶⁰

Recent years have witnessed a remarkable success of super-resolved fluorescence (FL) microscopy culminated in the awarding of 2014 Nobel Prize in Chemistry to Eric Betzig, Stefan Hell and William E. Moerner for their pioneering work. Fluorescence labelling allows “highlighting” and making visible subcellular structures; however it also has many drawbacks such as photobleaching and, most importantly, staining the biological samples with dyes is not always a desirable option.⁶¹ The label-free microscopy (LFM) relies on such effects as transient absorption⁶², super-oscillation⁶³, and hyperlens imaging⁶⁴. However, LFM is developing more slowly than FL microscopy for two reasons. First, the LFM mechanisms rely on much more subtle light-scattering processes in nanoscale objects that result in lower effective image contrasts. Second, the experimental quantification of resolution is complicated in LFM due to the lack of good “point”-sources.

Nanoscopy by microspheres emerged a surprisingly simple imaging technique⁶⁵ where a dielectric microsphere is placed in contact with the investigated object and its virtual image is observed using a conventional microscope, as shown in Figs. 23(a-c). It permits FL and LFM imaging. An important advancement in this area was a proposal of using high-index ($n \sim 2$) microspheres immersed in liquids or embedded in slabs,^{66,67} which made possible the application of this technology for imaging biomedical objects.^{68,69} Furthermore, imaging by high-index, liquid-immersed spheres resulted in higher-quality and better resolution images of nanoplasmonic structures.^{67,70,71}

To quantify the resolution in LFM methods, researchers often use larger-scale arrays containing objects with recognizable shape such as periodic stripes, stars, holes, dimers or

clusters.^{63,65,67,72} An idea of this approach is that the resolution can be estimated based on the minimal feature sizes which can be discerned in the optical images. For closely-spaced metallic cylinders (or holes) an edge-to-edge gap (g) is usually accepted as a resolution measure, see Fig. 1(d). We showed, however, that this approach can lead to overestimated resolution values. We developed more rigorous quantification of super-resolution based on a convolution of the arbitrarily shaped objects with the two-dimensional (2-D) point spread function (PSF).^{73,74,75,76} The proposed method can be viewed as an integral form of the super-resolution quantification accepted in FL microscopy where the PSF width can be narrower than the diffraction limit. As shown Figs. 23(e,f), we demonstrated imaging of metallic dimers and bowties with $\sim\lambda/7$ resolution, well in excess of the classical diffraction limit.

To develop a component for enhancing the microscope's resolution, we fabricated polydimethylsiloxane (PDMS) slabs with embedded high-index ($n \sim 2$) BaTiO₃ microspheres and showed for the first time that these slabs provide the optical super-resolution imaging combined with the surface scanning capability.⁷³⁻⁷⁵ As illustrated in Fig. 24(a), the PDMS slabs

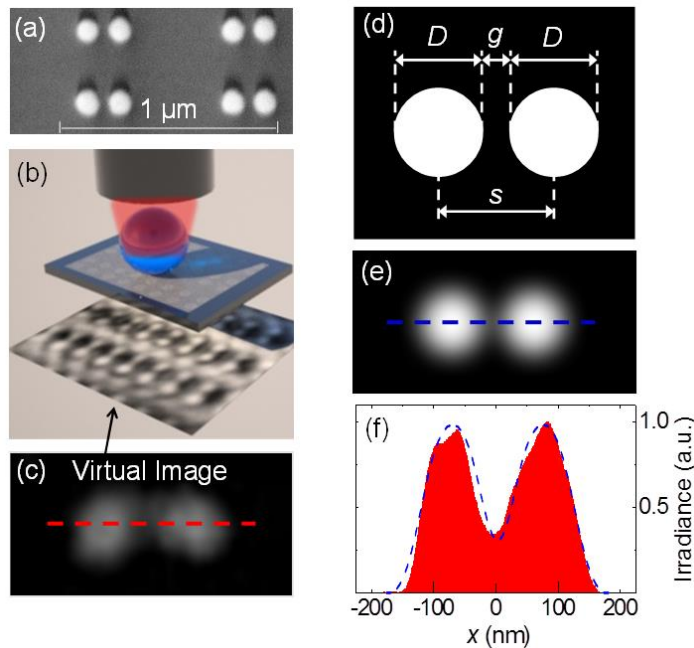


Fig. 23. (a) Array of Au dimers with $D=110$ nm and $g=40$ nm, (b) microscope setup, (c) virtual image, (d) drawn two-circle object, (e) convoluted image with the PSF width $\sim\lambda/7$, and (f) comparison of calculated (blue dashed lines) and measured at $\lambda=405$ nm (red profiles) image irradiance profiles.

adhere to the surface of nanoplasmonic structures which results in imaging of Au dimers and bowties with $\sim\lambda/6$ - $\lambda/7$ resolution. It is shown that the PDMS slabs can be translated along the surface of investigated samples after liquid lubrication. Initially, the resolution is diffraction limited; however the super-resolution gradually recovers as the lubricant evaporates. As illustrated in Fig. 24(b), we demonstrated that the microsphere-assisted imaging can be extended in a deep-UV range.⁷⁷ As shown in Fig. 24(c), the microfiber is another contact lens which provides magnification and super-resolution perpendicular to its axis. The resolution

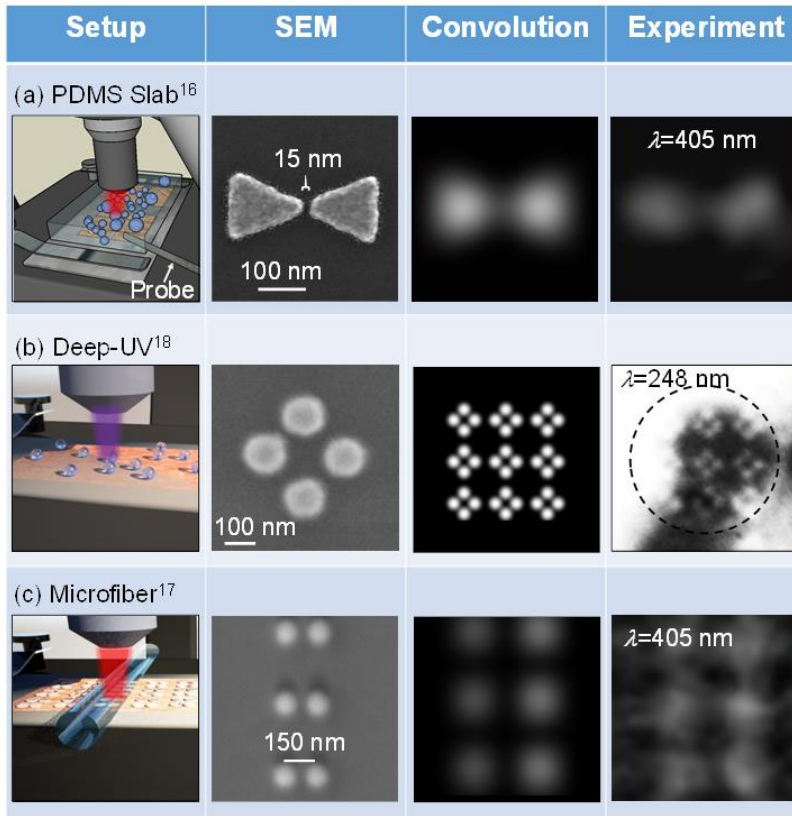


Fig. 24. (a) Experimental setup, SEM image of the object, convoluted and experimental images obtained through $4.5\ \mu\text{m}$ BaTiO_3 microsphere. The sphere is embedded in PDMS slab manipulated by the probe. (b) Same in the case of deep-UV imaging ($\lambda=248\ \text{nm}$) through $5\ \mu\text{m}$ SiO_2 sphere without PDMS slab. (c) Same in the case of imaging through SiO_2 microfiber with $D=12\ \mu\text{m}$.

was quantified based on the convolution of arbitrarily shaped objects with the PSF of cylindrical lens.⁷⁶ The resolution $\sim\lambda/6$ is demonstrated in the direction perpendicular to the fiber with hundreds of times larger field-of-view in comparison to microspheres.

Simplicity, massive impact on microscopy, and almost elusive origin of super-resolution by microspheres attracted a significant attention to its theoretical explanation. Initially, it was related to sharper than usual focusing of light by mesoscale spheres.⁶⁵ However, the width

of photonic jets is slightly less than $\lambda/2$ only in small microspheres with D about several λ .⁷⁸ The enhancement of focusing, therefore, seems to be insufficient to explain the super-resolution which is typically observed in larger spheres. The resonant excitation of whispering gallery modes can slightly improve the resolution⁷⁹ but their selective excitation is unlikely in the experiments with broad band illumination.

Recently, it was theoretically demonstrated⁸⁰ that the excitation of the electromagnetic modes of coupled metallic particles can facilitate their imaging. The 2-D model of imaging is shown in Fig. 25(a). One of the excited modes with antisymmetric distribution is modeled as a current source, $j(x)$, illustrated in Fig. 25(b). The magnified virtual images at various depth positions are seen in Fig. 25(c) significantly below the actual location of the current source. A zero-intensity minimum between the two particles is observable for any separations between the

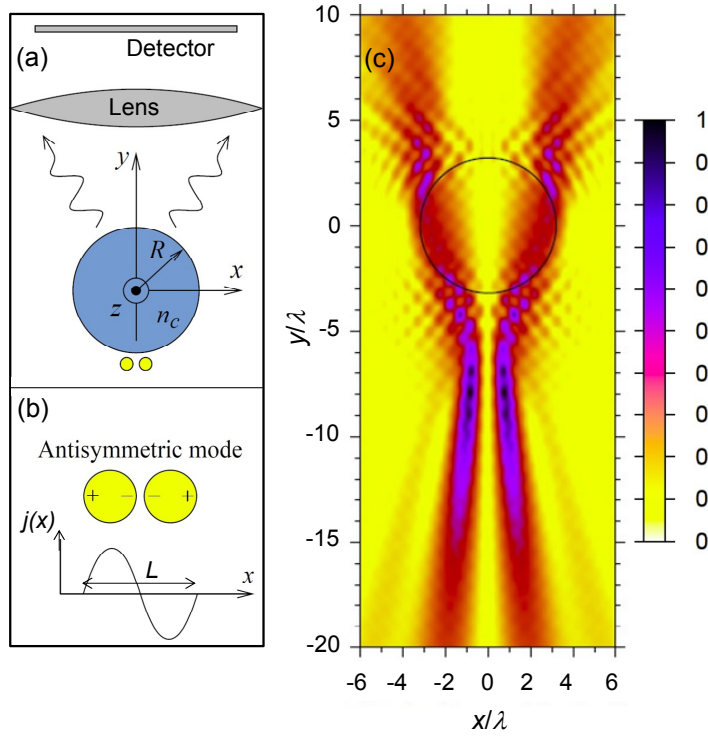


Fig. 25. (a) 2-D model⁸⁰ of imaging of two coupled particles by the dielectric cylinder with $n_c=1.4$ and $R=3.2\lambda$, (b) current source $j(x)$ with the length L representing antisymmetric mode, and (c) Virtual image intensities calculated as a function of the focusing depth (y) for $L=\lambda/2$.

particle centers. It takes place merely due to destructive interference of fields emitted from various points of the coherent current distribution. Although such images do not accurately display the shape of the objects, they allow a precise localization of such objects and can affect the quantification of resolution in the recent experiments with nanoplasmonic structures.

In summary, we have developed a rigorous analysis of resolution provided by microspheres and microfibers.^{75,76} We have synthesized transparent PDMS slabs that contain hundreds of embedded high-refractive-index barium titanate

microspheres. Such slabs, or coverslips, can be considered as a novel optical component for super-resolution microscopy that are usable in two different ways. First, without lubrication, they adhere to various surfaces and provide $\lambda/7$ resolution. Second, with liquid lubrication, the slabs become non-sticky and can be translated along a surface so that different spheres align with various objects. In future work we will explore the resolution limits of this technology in resonant nanoplasmonic and living subcellular structures. Various technologies and materials will be used for encapsulating high-index microspheres and microfibers. We will also develop commercial applications of these super-resolution technologies through our spin-off company SupriView.⁸¹

9. Enhancement of Sensitivity and Angle-of-View of Mid-IR Detectors

Enhancement of mid-wave infrared (MWIR) detectors and focal plane arrays (FPAs) constitute one more subject of this project. This direction was developed in collaboration with Air Force Research Laboratory. High performance MWIR FPAs are normally cooled to cryogenic temperatures in order to suppress the dark current noise.^{82,83} The operating temperature can be increased by minimizing the active volume of the detector that reduces the dark current. It has been achieved without degrading the light collection efficiency by designing photon trap structures such as photonic crystals⁸⁴ or textured surfaces with pyramidal relief features.⁸⁵ However, the angular operation range of such structures can be rather limited.

In this work, we realized MWIR photodetectors enhanced by photonic jets using microspheres made from sapphire ($n=1.71$), polystyrene ($n=1.56$), and soda-lime glass ($n=1.47$), with diameters in $20\lambda < D < 150\lambda$ range. Our initial proposal and preliminary results can be found elsewhere.^{86,87} The alignment of microspheres with the device mesas was controlled by the

virtual imaging through the spheres used as contact microlenses.

The results of our studies of integration microspheres with the individual photodetector mesas of MWIRs are published recently in Applied Physics Letters.⁸⁸ In this report, we will summarize our main observations without details. The integration of spheres with the photodetector mesas are illustrated in Fig. 26.

The study of the MWIR

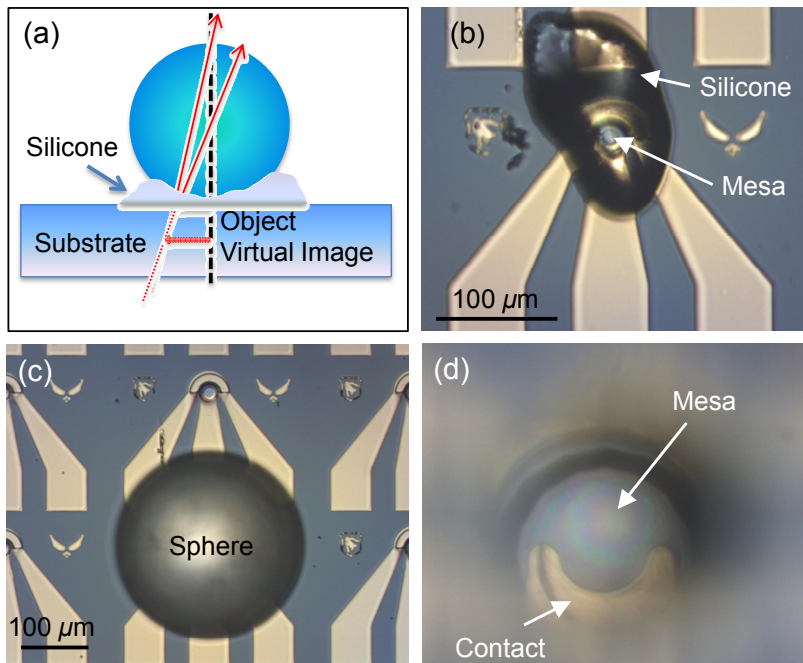


Fig. 26. Illustration of the microsphere integration with the photodetector mesa. (a) Virtual imaging geometry. Optical micrographs of (b) droplet of silicone used to attach the microsphere to the photodetector mesa, (c) microsphere at the top of the photodetector, and (d) virtual image of the photodetector mesa obtained through the sphere.

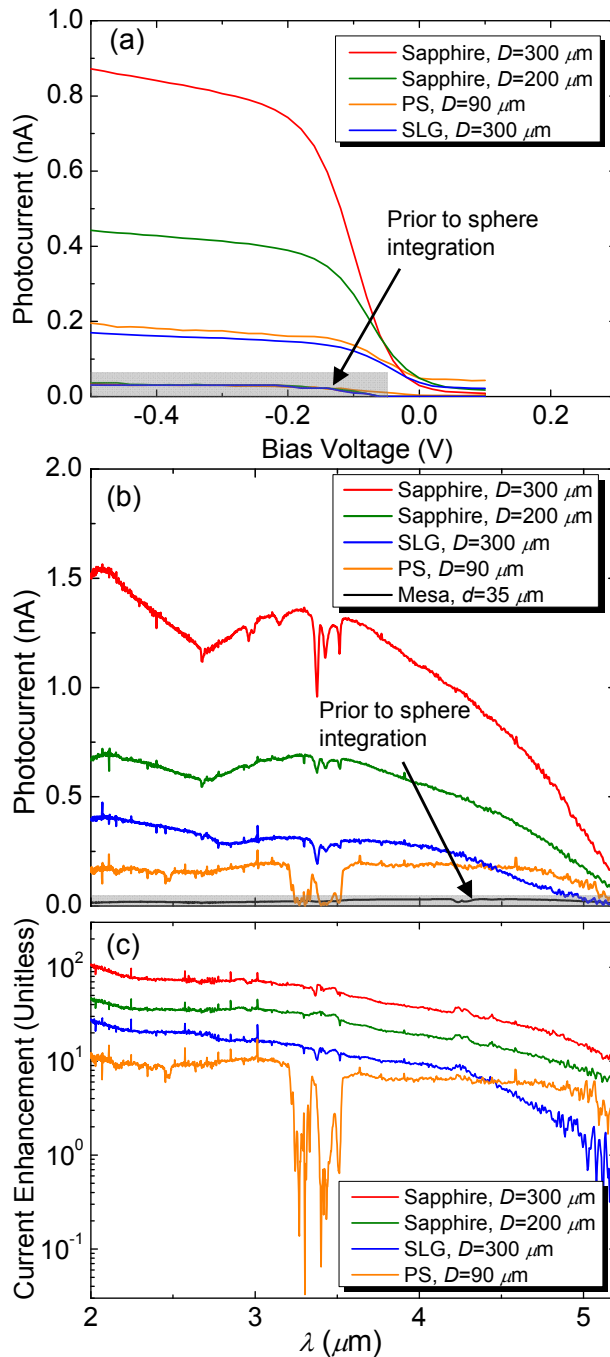


Fig. 27. (a) Photocurrent measured at different bias voltages from -0.5 to 0.1 V for $d=35\ \mu\text{m}$. (b) FTIR photocurrent spectra at a negative bias of 0.3 V with (colored curves) and without (black curve) the sphere. (c) Photocurrent enhancement factors, obtained by the division of FTIR photocurrent spectra at a negative bias of 0.3 V by the corresponding spectrum obtained without sphere.

response of detectors integrated with microspheres was performed by comparing the photocurrent response before and after integration. Prior to the integration of the microsphere, all of the individual SLS detectors were characterized. Photoresponse under different bias voltages at 80 K was measured using a beam with a half-angle of divergence about 3° obtained from a 500°C calibrated blackbody source with a narrow band filter ($\lambda=4.5\ \mu\text{m}$), shown within the grey box in Fig. 27(a) for a mesa with $d=35\ \mu\text{m}$. The angular acceptance of the detector integrated with microsphere is much larger than 3° with AOV being dependent on D , n , and on the shape of the microlens. The external quantum efficiency for these detectors at 80 K under a bias of -0.2 V is approximately 29% and it corresponds to about 40% of internal quantum efficiency.

The bias response of the same mesas integrated with sapphires ($D=200$ and $300\ \mu\text{m}$, $n=1.71$), polystyrene (PS, $D=90\ \mu\text{m}$, $n=1.56$), and soda-lime glass (SLG, $D=300\ \mu\text{m}$, $n=1.47$) microspheres is represented by the colored curves outside of the grey box in Fig. 27(a), indicating a significant photocurrent enhancement observed throughout the range of bias

voltages from -0.5 to 0.1 V.

As illustrated in Fig.27(b), the spectral response of the detectors was also measured before (black curve) and after (colored curves) integrating microspheres at -0.3 V bias, using a Fourier transform infrared (FTIR) spectrometer. Optical setup remained the same for blackbody photoresponse and photocurrent spectra measurements in Fig. 27. Blackbody photoresponse measurements in Fig. 27(a) were used to calibrate FTIR photocurrent spectra, in Fig. 27(b). The photocurrent enhancement is observed in Fig. 27(b) when photonic jets coupled to the photosensitive regions of the SLS detectors.

In conclusion, we showed that the performance of MWIR photodetectors can be dramatically enhanced by integration with dielectric microspheres. Our study is performed with single pixel detectors. Enhancing an entire FPA will require technologies of assembly of dielectric microspheres in large-scale arrays. To this end, many technologies can be used such as massively parallel manipulation with optoelectronic tweezers, self-assembly of microspheres on patterned electrodes by an applied electric field, templated self-assembly under dry conditions, and assembly of microspheres by air suction through array of micro holes. The choice of the optimal technology is determined by a specific application.

Experimentally, using photodetectors with $d=35\text{ }\mu\text{m}$, we demonstrated up to $100\times$ increase of sensitivity as a result of integration with $300\text{ }\mu\text{m}$ sapphire microspheres. Integration with microspheres would be even more advantages for smaller pixels. It should be noted, however, that the maximal advantage of this technology is expected in situations where the pixels are much smaller than the FPA pitch. This would permit simultaneous increase of collection efficiency and AOV. Using numerical modeling, we demonstrated that the back-illuminated structures with the thinned substrate have $\text{AOV}\sim 20^\circ$. Even larger AOVs can be achieved for front-illuminated FPAs integrated with microspheres.

10. Summary and Outlook

This project was devoted to all aspects of *microspherical photonics*, from technology to theory and applications. The term “microspherical photonics” was proposed by the PI to emphasize important role and some special features of this unusual branch of photonics which lies at the intersection soft condensed matter physics, applied physics, material science, optical engineering and optoelectronics. The dielectric microspheres are inexpensive and they be produced in massive quantities by using chemical or other methods. As classical “photonic atoms”, the microspheres have inevitable size and shape variations which do not allow their use in optoelectronic circuits with advanced functionalities. We showed in this project, however, that they can be sorted with extremely high uniformity of their internal optical resonances based on using resonant light forces. The sorted microspheres have uniformity of their WGM resonances on the order of $\sim 10^{-4}$ that is sufficient for developing a family of novel devices: coupled resonator optical waveguides, laser resonator arrays, sensors, etc.

The most interesting and promising direction of future research is related to use high-index microspheres with much more compact dimensions which will allow higher levels of integration and more advanced device applications. Developing this technology, however, will require some efforts because high-index microspheres have densities higher than the density of water. This means that the optical forces should be exerted differently in this case compared to water-immersed fiber couplers studied in this project. There are several ideas and principles which can be used for achieving high-volume sorting of high-index particles. One of these principles is based on developing an apparatus which would enable sorting of particles in air. Such particles can have typical diameters on the order of 2 microns and have Q-factors of their WGMs on the order of $\sim 10^4$. Sorting such particles would be quite challenging and we plan to submit our next ARO project devoted to this interesting problem.

Developing microsphere-chain waveguides in this project showed huge potential of microspherical photonics for developing practical applications. We demonstrated low-loss waveguides with unusual periodical focusing capability. We observed unusual polarization-filtering properties of such chains. It is interesting that they filter radially-polarized modes which can be focused to smaller spots compared to unpolarized or linearly polarized beams. We demonstrated applications of this technology in ultra-precise laser-tissue surgery. These applications have a significant prospect of commercialization. It already resulted in securing NIH

funding for our collaborative STTR Phase I project. Generally, this research brings about issues of integration of chains of spheres with different laser sources and flexible optical delivery systems used in practical surgical applications. We developed and realized some of these designs and tested our laser scalpels ex-vivo.

Optical super-resolution is a fantastic application of microspherical photonics. In our project, we developed the most important direction of this research dealing with high-index microspheres immersed in liquids or embedded in elastomeric slabs. This is the most important direction because it opens up a prospect for the biomedical applications of this technology. This area is also very interesting from the fundamental point of view. Nanoplasmonic aspects of super-resolution mechanism are still not completely understood at the present time. They are related to areas of nanoplasmonic antennas, metallo-dielectric antennas, and super-gain antennas. The main issue is that antenna and imaging applications of nanoplasmonics are related. However, such aspects as mechanisms of image formation on resonance with WGMs in spheres, coherent and incoherent imaging mechanisms, role of collective plasmonic excitations and role of spatial dispersion still await new fundamental breakthrough studies. In our research, we mainly modeled point-dipoles as objects. However, nanoplasmonic objects are more complicated than point objects. It is likely that these differences can provide keys for a question about fundamental origins of super-resolution in these structures. However, it needs to be seen if a picture of propagating plasmon-polariton waves or a picture of localized surface plasmon resonances is more adequate. It seems that label-free super-resolution is becoming a new frontier in photonics.

Enhancement of MWIR detectors by microspheres observed in this work is another strong application of microspherical photonics. It does not require extremely precise size or shape sorting of microspheres. However, for integrating this technology in large FPAs, the techniques of assembly of microspheres in large arrays should be developed. In our very recent work we show that it can be achieved using assembly of microspheres by air suction through array of micro holes. First results demonstrated less than $\sim 1\%$ of error-rate in arrangement of microspheres. Transferring of such ordered arrays onto the surface of FPA can be performed by using mask aligners and layers of photoresist which can be used to fix dielectric microspheres in positions centered with corresponding device mesas. A combination of enhanced sensitivity, increased angle-of-view, and reduced dark current and increased operational temperature is unique for a technology of integration with microspheres proposed and developed in this project.

11. Bibliography

-
- ¹ Y. Liu and X. Zhang, “Metamaterials: a new frontier of science and technology,” *Chem. Soc. Rev.* **40**, 2494–2507 (2011).
- ² V. N. Astratov, V. N. Bogomolov, A. A. Kaplyanskii, A. V. Prokofiev, L.A. Samoilovich, S.M. Samoilovich, and Y.A. Vlasov, “Optical spectroscopy of opal matrices with CdS embedded in its pores: quantum confinement and photonic band gap effects,” *Nuovo Cimento D* **17**, 1349-1354 (1995).
- ³ V. N. Astratov, Y. A. Vlasov, O. Z. Karimov, A. A. Kaplyanskii, Y. G. Musikhin, N. A. Bert, V. N. Bogomolov, and A. V. Prokofiev, “Photonic band gaps in 3D ordered FCC silica matrices,” *Phys. Lett. A* **222**, 349-353 (1996); “Photonic band structure of 3D ordered silica matrices,” *Superlattices & Microstruct.* **22**, 393-397 (1997).
- ⁴ Y. A. Vlasov, V. N. Astratov, O. Z. Karimov, A. A. Kaplyanskii, V. N. Bogomolov, and A. V. Prokofiev, “Existence of a photonic pseudogap for visible light in synthetic opals,” *Phys. Rev. B* **55**, R13357-R13360 (1997).
- ⁵ Y. A. Vlasov, V. N. Astratov, A. V. Baryshev, A. A. Kaplyanskii, O. Z. Karimov, and M. F. Limonov, “Manifestation of intrinsic defects in the optical properties of self-organized opal photonic crystals,” *Phys. Rev. E* **61**, 5784-5793 (2000).
- ⁶ V. N. Astratov, A. M. Adawi, M. S. Skolnick, V. K. Tikhomirov, V. Lyubin, D. G. Lidzey, M. Ariu, and A. L. Reynolds, “Opal photonic crystals infiltrated with chalcogenide glasses,” *Appl. Phys. Lett.* **78**, 4094-4096 (2001).
- ⁷ V. N. Astratov, A. M. Adawi, S. Fricker, M. S. Skolnick, D. M. Whittaker, and P. N. Pusey, “Interplay of order and disorder in the optical properties of opal photonic crystals,” *Phys. Rev. B* **66**, 165215 (2002).
- ⁸ V. N. Astratov, R. M. Stevenson, M. S. Skolnick, D. M. Whittaker, S. Brand, I. Culshaw, T. F. Krauss, R. M. De La Rue, and O. Z. Karimov, “Experimental technique to determine the band structure of two-dimensional photonic lattices,” *Proc. IEE Optoelectron.*, **145**, 398-402 (1998).
- ⁹ V. N. Astratov, I. S. Culshaw, R. M. Stevenson, D. M. Whittaker, M. S. Skolnick, T. F. Krauss, and R. M. De La Rue, “Resonant coupling of near-infrared radiation to photonic band structure waveguides,” *J. Lightwave Technol.* **17**, 2050-2057 (1999).
- ¹⁰ V. N. Astratov, D. M. Whittaker, I. S. Culshaw, R. M. Stevenson, M. S. Skolnick, T. F. Krauss, and R. M. De La Rue, “Photonic band structure effects in the reflectivity of periodically patterned waveguides,” *Phys. Rev. B* **60**, R16255-R16258 (1999).
- ¹¹ V. N. Astratov, R. M. Stevenson, I. S. Culshaw, D. M. Whittaker, M. S. Skolnick, T. F. Krauss, and R. M. De La Rue, “Heavy photon dispersions in photonic crystal waveguides,” *Appl. Phys. Lett.* **77**, 178-180 (2000).

-
- ¹² D. M. Whittaker, I. S. Culshaw, V. N. Astratov, and M. S. Skolnick, "Photonic bandstructure of patterned waveguides with dielectric and metallic cladding," *Phys. Rev. B*, 073102 (2002).
- ¹³ A. D. Bristow, V. N. Astratov, R. Shimada, I. S. Culshaw, M. S. Skolnick, D. M. Whittaker, A. Tahraoui, and T. F. Krauss, "Polarization conversion in the reflectivity properties of photonic crystal waveguides," *IEEE J. of Q. El.* **38**, 880-884 (2002).
- ¹⁴ A. D. Bristow, D. M. Whittaker, V. N. Astratov, M. S. Skolnick, A. Tahraoui, T. F. Krauss, M. Hopkinson, M. P. Groucher, and G. A. Gehring, "Defect states and commensurability in dual-period $\text{Al}_x\text{Ga}_{1-x}\text{As}$ photonic crystal waveguides," *Phys. Rev. B* **68**, 033303 (2003).
- ¹⁵ A. Armitage, M. S. Skolnick, V. N. Astratov, D. M. Whittaker, G. Panzarini, L. C. Andreani, T. F. Fisher, J. S. Roberts, A. V. Kavokin, M. S. Kaliteevski, and M. R. Vladimirova, "Optically induced splitting of bright excitonic states in coupled quantum microcavities," *Phys. Rev. B* **57**, 14877-14881 (1998).
- ¹⁶ M. Emam-Esmail, V. N. Astratov, M. S. Skolnick, D. M. Whittaker, and J. S. Roberts, "Asymmetric photoluminescence spectra from excitons in a coupled microcavity," *Phys. Rev. B* **62**, 1552-1555 (2000).
- ¹⁷ R. M. Stevenson, V. N. Astratov, M. S. Skolnick, D. M. Whittaker, M. Emam-Ismael, A. I. Tartakovskii, P. G. Savvidis, J. J. Baumberg and J. S. Roberts, "Continuous wave observation of massive polariton redistribution by stimulated scattering in semiconductor microcavities," *Phys. Rev. Lett.* **85**, 3680-3683 (2000).
- ¹⁸ R. M. Stevenson, V. N. Astratov, M. S. Skolnick, J. S. Roberts and G. Hill, "Uncoupled excitons in semiconductor microcavities detected in resonant Raman scattering," *Phys. Rev. B* **67**, 081301(R) (2003).
- ¹⁹ V. N. Astratov, J. P. Franchak, and S. P. Ashili, "Optical coupling and transport phenomena in chains of spherical dielectric microresonators with size disorder," *Appl. Phys. Lett.* **85**, 5508-5510 (2004).
- ²⁰ S. Deng, W. Cai, and V. N. Astratov, "Numerical study of light propagation via whispering gallery modes in microcylinder coupled resonator optical waveguides," *Opt. Express* **12**, 6468-6480 (2004).
- ²¹ A. V. Kanaev, V. N. Astratov, and W. Cai, "Optical coupling at a distance between detuned spherical cavities," *Appl. Phys. Lett.* **88**, 111111 (2006).
- ²² S. P. Ashili, V. N. Astratov, and E. C. H. Sykes, "The effects of inter-cavity separation on optical coupling in dielectric bispheres," *Opt. Express* **14**, 9460-9466 (2006).
- ²³ V. N. Astratov, and S. P. Ashili, "Percolation of light through whispering gallery modes in 3D lattices of coupled microspheres," *Opt. Express* **15**, 17351-17361 (2007).
- ²⁴ B. E. Little, S. T. Chu, H. A. Haus, J. Foresi, and J.-P. Laine, "Microring resonator channel dropping filters," *J. of Lightwave Technol.* **15**, 998-1005 (1997).

-
- ²⁵ B. E. Little, S. T. Chu, P. P. Absil, J. V. Hryniewicz, F. G. Johnson, F. Seiferth, D. Gill, V. Van, O. King, and M. Trakalo, "Very high-order microring resonator filters for WDM applications," *IEEE Photon. Technol. Lett.* **16**, 2263-2265 (2004).
- ²⁶ J. K. S. Poon, L. Zhu, G. A. DeRose, and A. Yariv, "Transmission and group delay of microring coupled-resonator optical waveguides," *Opt. Lett.* **31**, 456-458 (2006).
- ²⁷ A. M. Kapitonov and V. N. Astratov, "Observation of nanojet-inducing modes with small propagation losses in chains of coupled spherical cavities," *Opt. Lett.* **32**, 409-411 (2007).
- ²⁸ S. Yang and V. N. Astratov, "Photonic nanojet-induced modes in chains of size-disordered microspheres with an attenuation of only 0.08 dB per sphere," *Appl. Phys. Lett.* **92**, 261111 (2008).
- ²⁹ Z. Chen, A. Taflove, and V. Backman, "Photonic nanojet enhancement of backscattering of light by nanoparticles: a potential novel visible-light ultramicroscopy technique," *Opt. Express* **12**, 1214-1220 (2004).
- ³⁰ P. Ferrand, J. Wenger, A. Devilez, M. Pianta, B. Stout, N. Bonod, E. Popov, and H. Rigneault, "Direct imaging of photonic nanojets," *Opt. Express* **16**, 6930-6940 (2008).
- ³¹ S. Yang and V. N. Astratov, "Spectroscopy of coherently coupled whispering-gallery modes in size-matched bispheres assembled on a substrate," *Opt. Lett.* **34**, 2057-2059 (2009).
- ³² V.N. Astratov, S. Yang, S. Lam, B.D. Jones, D. Sanvitto, D.M. Whittaker, A.M. Fox, and M.S. Skolnick, A. Tahraoui, P.W. Fry, and M. Hopkinson, "Whispering Gallery Resonances in Semiconductor Micropillars," *Appl. Phys. Lett.* **91**, 071115 (2007).
- ³³ B.D. Jones, M. Oxborrow, V.N. Astratov, M. Hopkinson, A. Tahraoui, M.S. Skolnick, and A.M. Fox, "Splitting and Lasing of Whispering Gallery Modes in Quantum Dot Micropillars," *Opt. Express* **18**, 22578-22592 (2010).
- ³⁴ O. Svitelskiy, Y. Li, A. Darafsheh, M. Sumetsky, D. Carnegie, E. Rafailov, and V.N. Astratov, "Fiber coupling to BaTiO₃ glass microspheres in an aqueous environment," *Opt. Lett.* **36**, 28622865 (2011).
- ³⁵ A. Ashkin and J. M. Dziedzic, *Phys. Rev. Lett.* **38**, 1351-1354 (1977).
- ³⁶ Y. Li, O. V. Svitelskiy, A. V. Maslov, D. Carnegie, E. Rafailov, and V. N. Astratov, "Giant resonant light forces in microspherical photonics," *Light: Science and Applications* **2**, e64 (2013).
- ³⁷ A. V. Maslov, V. N. Astratov, and M. I. Bakunov, "Resonant propulsion of a microparticle by a surface wave," *Phys. Rev. A* **87**, 053848 (2013).
- ³⁸ V. N. Astratov, Y. Li, O. V. Svitelskiy, A. V. Maslov and M. I. Bakunov, D. Carnegie and E. Rafailov, "Microspherical photonics: Ultra-high resonant propulsion forces," December issue of *Optics and Photonics News* (2013).

-
- ³⁹ Y. Li, A.V. Maslov, N.I. Limberopoulos, A.M. Urbas, and V.N. Astratov, "Spectrally resolved resonant propulsion of dielectric microspheres," *Laser & Photonics Rev.* **9**, 263–273 (2015).
- ⁴⁰ A.V. Maslov and V.N. Astratov, "Microspherical photonics: sorting resonant photonics atoms by using light, *Appl. Phys. Lett.* **105**, 121113 (2014).
- ⁴¹ V. N. Astratov, "Fundamentals and applications of microsphere resonator circuits, " *Photonic Microresonator Research and Applications*, Springer Series in Optical Sciences Vol. 156, edited by I. Chremmos, O. Schwelb, and N. Uzunoglu (Springer, New York, 2010), Ch. 17, pp. 423-457.
- ⁴² T. Mitsui, Y. Wakayama, T. Onodera, Y. Takaya, and H. Oikawa, "Observation of light propagation across a 90° corner in chains of microspheres on a patterned substrate," *Opt. Lett.* **33**, 1189-1191 (2008).
- ⁴³ Y. Hara, T. Mukaiyama, K. Takeda, and M. Kuwata-Gonokami, "Heavy photon states in photonic chains of resonantly coupled cavities with supermonodispersive microspheres," *Phys. Rev. Lett.* **94**, 203905 (2005).
- ⁴⁴ T. Mitsui, Y. Wakayama, T. Onodera, T. Hayashi, N. Ikeda, Y. Sugimoto, T. Takamasu, and H. Oikawa, "Micro-demultiplexer of coupled resonator optical waveguide fabricated by microspheres," *Adv. Mater.* **22**, 3022-3026 (2010).
- ⁴⁵ O. Lecarme, T. Pinedo-Rivera, L. Arbes, T. Honegger, K. Berton, and D. Peyrade, "Colloidal optical waveguides with integrated local light sources built by capillary force assembly," *J. Vac. Sci. Technol. B* **28**, C6O11-C6O15 (2010).
- ⁴⁶ T. Mitsui, T. Onodera, Y. Wakayama, T. Hayashi, N. Ikeda, Y. Sugimoto, T. Takamasu, and H. Oikawa, "Influence of micro-joints formed between spheres in coupled-resonator optical waveguide," *Opt. Express* **19**, 22258-22267 (2011).
- ⁴⁷ A. K. Tiwari, R. Uppu and S. Mujumdar, "Experimental demonstration of small-angle bending in an active direct-coupled chain of spherical microcavities," *Appl. Phys. Lett.* **103**, 171108 (2013).
- ⁴⁸ A. Darafsheh and V. N. Astratov, "Periodically focused modes in chains of dielectric spheres," *Appl. Phys. Lett.* **100**, 061123 (2012).
- ⁴⁹ A. Darafsheh, A. Fardad, N. M. Fried, A. N. Antoszyk, H. S. Ying, and V. N. Astratov, "Contact focusing multimodal microprobes for ultraprecise laser tissue surgery," *Opt. Express* **19**, 3440-3448 (2011).
- ⁵⁰ K. W. Allen, A. Darafsheh, F. Abolmaali, N. Mojaverian, N. I. Limberopoulos, A. Lupu, and V. N. Astratov, "Microsphere-chain waveguides: Focusing and transport properties," *Appl. Phys. Lett.* **105**, 021112 (2014).
- ⁵¹ M. Sumetsky, "How thin can a microfiber be and still guide light?" *Opt. Lett.* **31**, 870-872 (2006).
- ⁵² A. Darafsheh, N. I. Limberopoulos, A. Lupu, and V. N. Astratov, "Filtering of radially polarized beams by microsphere-chain waveguides," *Proc. of SPIE* 2013, paper 8627-13, 7 pp. Phot. West, San Francisco, Feb. 3-7 (2013).

-
- ⁵³ A. Darafsheh, N. Mojaverian, N. I. Limberopoulos, K. W. Allen, A. Lupu, and V. N. Astratov, "Formation of polarized beams in chains of dielectric spheres and cylinders," *Opt. Lett.* **38**, 4208-4211 (2013).
- ⁵⁴ E. Hecht, *Optics*, 4th Ed., Addison-Wesley (Reading, 2001).
- ⁵⁵ A. Al-Qasimi, O. Korotkova, D. James, and E. Wolf, "Definitions of the degree of polarization of a light beam," *Opt. Lett.* **32**, 1015-1016 (2007).
- ⁵⁶ V.N. Astratov, "Focusing multimodal optical microprobe devices and methods," U.S. patent 8,554,031 B2 published on 08 October 2013 (priority date January 17, 2009).
- ⁵⁷ V.N. Astratov, "Contact Focusing Hollow-Core Fiber Microprobes," U.S. patent application 2015/0316717 A1 published on November 5, 2015, related to U.S. provisional application 61/728,835 filed on 11/21/2012.
- ⁵⁸ T. C. Hutchens, A. Darafsheh, A. Fardad, A. N. Antoszyk, H. S. Ying, V. N. Astratov, and N. M. Fried, "Characterization of novel microsphere chain fiber optic tips for potential use in ophthalmic laser surgery," *J. Biomed. Opt.* **17**, 068004 (2012).
- ⁵⁹ T.C. Hutchens, A. Darafsheh, A. Fardad, A.N. Antoszyk, H.S. Ying, V.N. Astratov, and N.M. Fried, "Detachable Microsphere Scalpel Tips for Potential Use in Ophthalmic Surgery with the Erbium:YAG laser," *J. Biomed. Opt.* **19**, 018003 (2014).
- ⁶⁰ S. W. Hell, "Nanoscopy with focused light," *Ann. Phys. (Berlin)* **527**, pp. 423-445 (2015).
- ⁶¹ S. Weisenburger and V. Sandoghdar, Light microscopy: an ongoing contemporary revolution, *Contemporary Physics* **56**, pp. 123-143 (2015).
- ⁶² P. Wang, M.N. Slipchenko, J. Mitchell, C. Yang, E.O. Potma, X. Xu, and J.-X. Cheng, "Far-field imaging of non-fluorescent species with subdiffraction resolution," *Nat. Phot.* **7**, 449-453 (2013).
- ⁶³ E.T.F. Rogers, J. Lindberg, T. Roy, S. Savo, J.E. Chad, M.R. Dennis, and N.I. Zheludev, "A super-oscillatory lens optical microscope for subwavelength imaging," *Nat. Mater.* **11**, 432-435 (2012).
- ⁶⁴ Z. Jacob, L. V. Alekseyev and E. Narimanov, "Optical Hyperlens: Far-field imaging beyond the diffraction limit," *Opt. Express* **14**, 8247-8256 (2006).
- ⁶⁵ Z. Wang, W. Guo, L. Li, B. Luk'yanchuk, A. Khan, Z. Liu, Z. Chen, and M. Hong, "Optical virtual imaging at 50 nm lateral resolution with a white-light nanoscope," *Nat. Commun.* **2**, 218 (2011).
- ⁶⁶ V. N. Astratov and A. Darafsheh, "Methods and systems for super-resolution optical imaging using high-index of refraction microspheres and microcylinders," US patent application 2014/0355108 A1 published on December 4, 2014, related to US provisional application 61/656,710 filed on June 7, 2012. <http://www.freepatentsonline.com/20140355108.pdf>
- ⁶⁷ A. Darafsheh, G. F. Walsh, L. Dal Negro, and V. N. Astratov, "Optical super-resolution by high-index liquid-immersed microspheres," *Appl. Phys. Lett.* **101**, 141128 (2012).
- ⁶⁸ L. Li, W. Guo, Y. Yan, S. Lee and T. Wang, "Label-free super-resolution imaging of adenoviruses by submerged microsphere optical nanoscopy," *Light: Science & Applications* **2**, e104 (2013).
- ⁶⁹ H. Yang, N. Moullan, J. Auwerx, and M. A. M. Gijs, "Super-resolution biological microscopy using virtual imaging by a microsphere nanoscope," *Small* **10**, pp. 1712-1718 (2014).
- ⁷⁰ L. A. Krivitsky, J. J. Wang, Z. Wang, and B. Luk'yanchuk, "Locomotion of microspheres for super-resolution imaging," *Sci. Reports* **3**, 3501 (2013).

-
- ⁷¹ A. Darafsheh, N. I. Limberopoulos, J. S. Derov, D. E. Walker, Jr., and V. N. Astratov, “Advantages of microsphere-assisted super-resolution imaging technique over solid immersion lens and confocal microscopies,” *Appl. Phys. Lett.* **104**, 061117 (2014).
- ⁷² Y. Yan, L. Li, C. Feng, W. Guo, S. Lee, and M. Hong, “Microsphere-coupled scanning laser confocal nanoscope for sub-diffraction-limited imaging at 25 nm lateral resolution in the visible spectrum,” *ACS Nano* **8**, pp. 1809-1816 (2014).
- ⁷³ K. W. Allen, N. Farahi, Y. Li, N. I. Limberopoulos, D. E. Walker Jr., A. M. Urbas, and V. N. Astratov, “Super-resolution imaging by arrays of high-index spheres embedded in transparent matrices,” *IEEE Proc. of Aerospace and Electronics Conference (NAECON)*, Dayton, June 24-27 (2014), pp. 50-52. <http://arxiv.org/abs/1412.1873>
- ⁷⁴ K. W. Allen, “Waveguide, photodetector, and imaging applications of microspherical photonics,” Ph.D. dissertation (University of North Carolina at Charlotte, Oct. 2014), Chapter 4: Super-Resolution Imaging through Arrays of High-Index Spheres Embedded in Transparent Matrices, pp. 98-122. <http://gradworks.umi.com/36/85/3685782.html>
- ⁷⁵ K. W. Allen, N. Farahi, Y. Li, N. I. Limberopoulos, D. E. Walker, Jr., A. M. Urbas, V. Liberman, and V. N. Astratov, “Super-resolution microscopy by movable thin-films with embedded microspheres: Resolution analysis,” *Ann. Phys. (Berlin)* **527**, pp. 513–522 (2015).
- ⁷⁶ K. W. Allen, N. Farahi, Y. Li, N. I. Limberopoulos, D. E. Walker Jr., A. M. Urbas, and V.N. Astratov, “Overcoming the diffraction limit of imaging nanoplasmonic arrays by microspheres and microfibers,” *Opt. Express* **23**, pp. 24484-24496 (2015).
- ⁷⁷ K. W. Allen, V. Liberman, M. Rothschild, N. I. Limberopoulos, D. E. Walker Jr., A. M. Urbas, and V. N. Astratov, “Deep-UV microsphere-assisted ultramicroscopy,” in *Proceedings of IEEE 17th International Conference on Transparent Optical Networks–ICTON* (IEEE, 2015), Paper No. We.P.26.
- ⁷⁸ X. Li, Z. Chen, A. Taflove, and V. Backman, “Optical analysis of nanoparticles via enhanced backscattering facilitated by 3-D photonic nanojets,” *Opt. Express* **13**, pp. 526-533 (2005).
- ⁷⁹ T. X. Hoang, Y. Duan, X. Chen, and G. Barbastathis, “Focusing and imaging in microsphere-based microscopy,” *Opt. Express* **23**, 12337-12353 (2015).
- ⁸⁰ A. V. Maslov and V. N. Astratov, “Imaging of sub-wavelength structures radiating coherently near microspheres,” *Appl. Phys. Lett.* **108**, 051104 (2016).
- ⁸¹ <http://startupcompete.co/startup-idea/life-sciences-materials/surpriviewmicroscope-attachment/38861> Startup challenge competition at Photonics West 2016. Accessed 19 January 2016.
- ⁸² A. Rogalski, “Progress in focal plane array technologies,” *Progress in Quantum Electronics* **36**, 342–473 (2012).
- ⁸³ N.K. Dhar, R. Dat, and A.K. Sood, *Optoelectronics – Advanced Materials and Devices*, edited by S.L. Pyshkin and J.M. Ballato (InTech, open access publisher, 2013), Ch. 7, pp. 149-190.
- ⁸⁴ K.D. Smith, J.G.A. Wehner, R.W. Graham, J.E. Randolph, A.M. Ramirez, G.M. Venzor, K. Olsson, M.F. Vilela, and E.P.G. Smith, “High operating temperature mid-wavelength infrared HgCdTe photon trapping focal plane arrays,” *Proc. SPIE* **8353**, 83532R (2012).
- ⁸⁵ A.I. D’Souza, E. Robinson, A.C. Ionescu, D. Okerlund, T.J. de Lyon, R.D. Rajavel, H. Sharifi, D. Yap, N. Dhar, P.S. Wijewarnasuriya, and C. Grein, “MWIR InAs1-xSbx nCBn Detectors Data and Analysis,” *Proc. SPIE* **8353**, 835333 (2012).
- ⁸⁶ V.N. Astratov, K.W. Allen, N.I. Limberopoulos, A. Urbas, and J.M. Duran, “Photodetector focal plane array systems and methods,” patent application 14/587,068 filed on 12/31/2014. U.S. patent 9,362,324 (7 June 2016).
- ⁸⁷ K.W. Allen, J.M. Duran, G. Ariyawansa, N.I. Limberopoulos, A.M. Urbas, and V.N. Astratov, “Photonic Jets for Strained-Layer Superlattice Infrared Photodetector Enhancement,” in *IEEE*

Proceedings of National Aerospace and Electronics Conference, Dayton, Ohio, 25-27 June 2014 (IEEE 2014), pp.32-33.

⁸⁸ K.W. Allen, F. Abolmaali, J.M. Duran, G. Ariyawansa, N.I. Limberopoulos, A.M. Urbas, and V.N. Astratov, "Increasing Sensitivity and Angel-of-View of Mid-Wave Infrared Detectors by Integration with Dielectric Microspheres," *Appl. Phys. Lett.* **108**, 241108 (2016).